The Interdisciplinary Sciences Journal

TCABSE-J

ISSN: 2583-2557 Volume 1 Issue 6 Oct 24th, 2023

H. pylori infected antrum Biopsy in BHI Broth

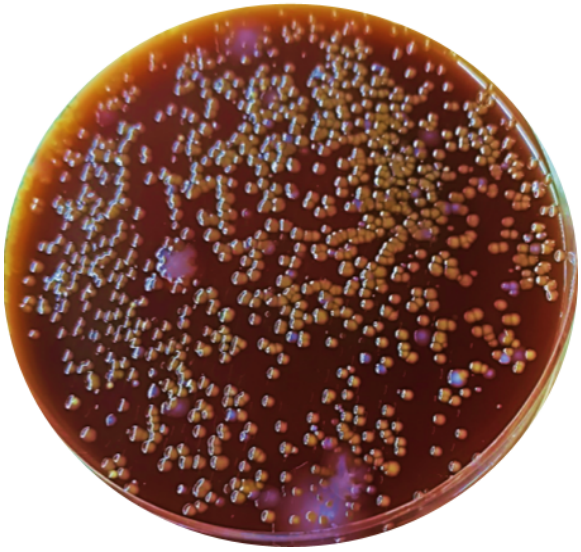

H. pylori

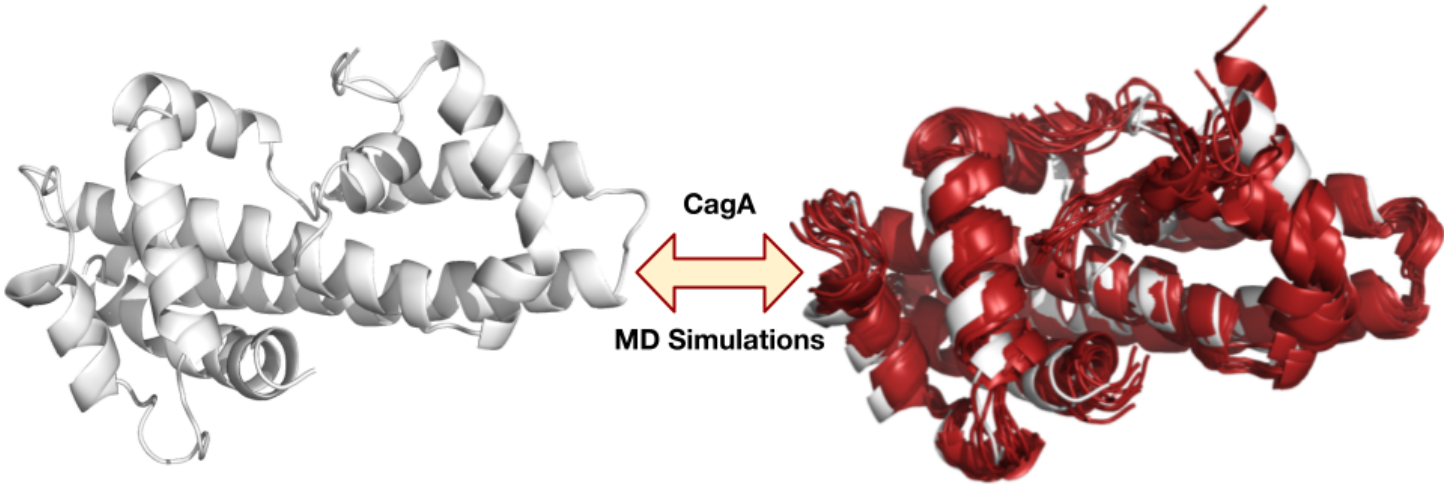

The Center for Advanced-Applied Biological Sciences & Entrepreneurship (TCABS-E). Rajamahendravaram. India.

Table of Contents

TCABSE-J Communications
ISSN: 2583- 2557, *Volume 1, Issue 6, pp1-3. 2023.*

TCABSE-J Interdisciplinary Sciences Journal

An intermittent culturing protocol for *Helicobacter pylori* from clinical biopsies

Madhumita Aggunna[1], Ramesh Reddy[2], Girinadh R. S. Lekkala[2] and Ravikiran S. Yedidi[1, 3, *]

[1]Department of Intramural research core, The Center for Advanced-Applied Biological Sciences & Entrepreneurship (TCABS-E), Visakhapatnam 530016, A.P. India; [2]Department of Gastroenterology, Andhra Medical College, King George Hospital, Visakhapatnam 531011, A. P. India; [3]Department of Zoology, Andhra University, Visakhapatnam 530003, A. P. India. (*Correspondence to R.S.Y.: tcabse.india@gmail.com).

Keywords: *Helicobacter pylori*, Brain Heart Infusion (BHI) broth, BHI blood agar, oxygen detector tablets, Microaerophilic conditions, Anaerobic gas packs, gastric ulcers and gastric cancers.

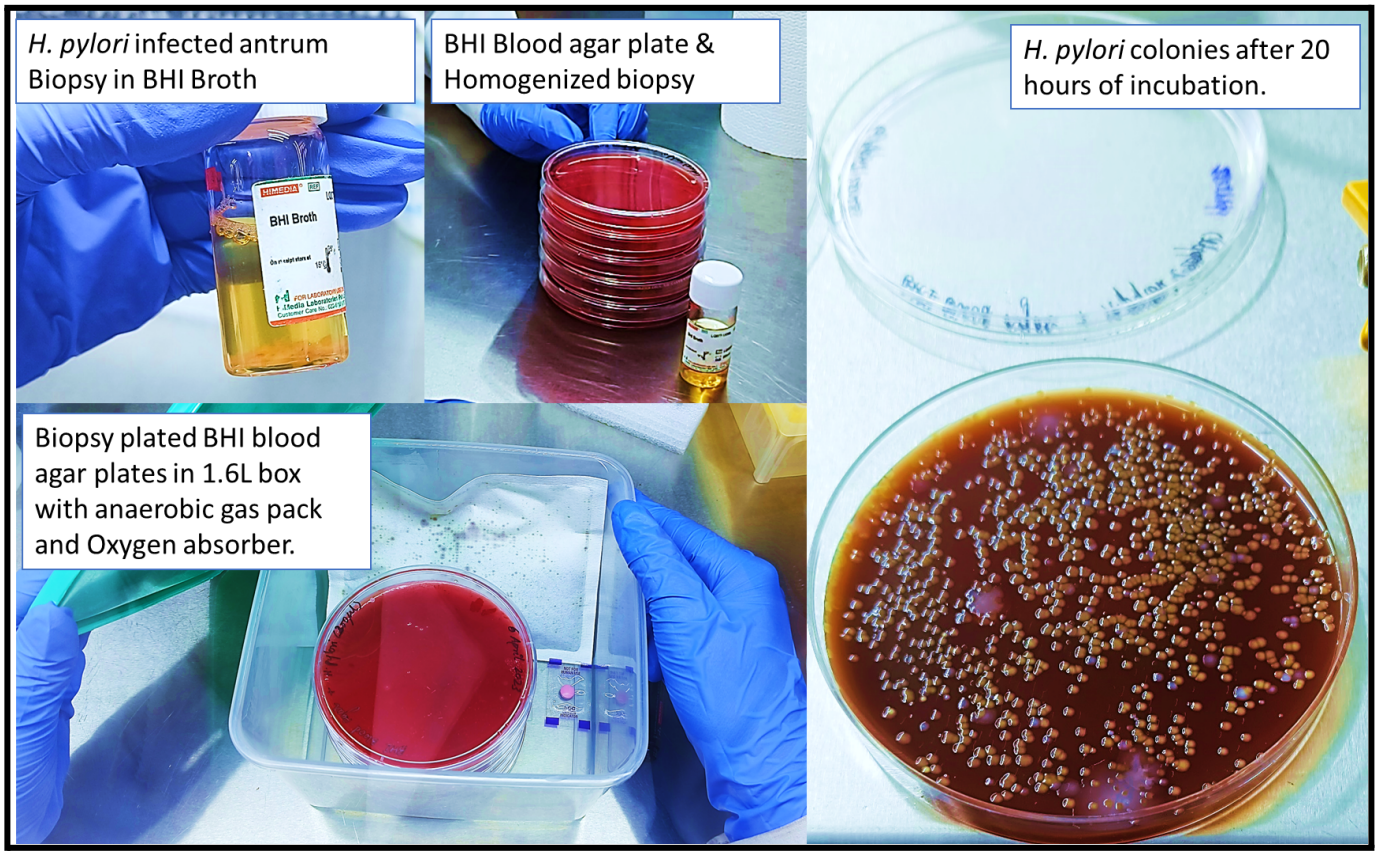

Figure 1. Obtaining *H. pylori* colonies from the antrum biopsy in the BHI blood agar plates. Biopsies were directly collected into the BHI broth (top left panel) and were plated on the BHI Blood agar plates (top middle panel). Plates were incubated in microaerobic conditions using a gas pack (bottom left panel) for 20 hours to obtain the bacterial colonies (right panel).

Citation: Aggunna, M., Reddy, R., Lekkala, G.R.S. and Yedidi, R.S. (2023). An intermittent culturing protocol for *Helicobacter pylori* from the clinical biopsies. *TCABSE-J*, Vol. 1, Issue 6:1-3. Epub: Apr 8th, 2023.

TCABSE-J Communications
ISSN: 2583- 2557, *Volume 1, Issue 6, pp1-3. 2023.*

TCABSE-J
Interdisciplinary Sciences Journal

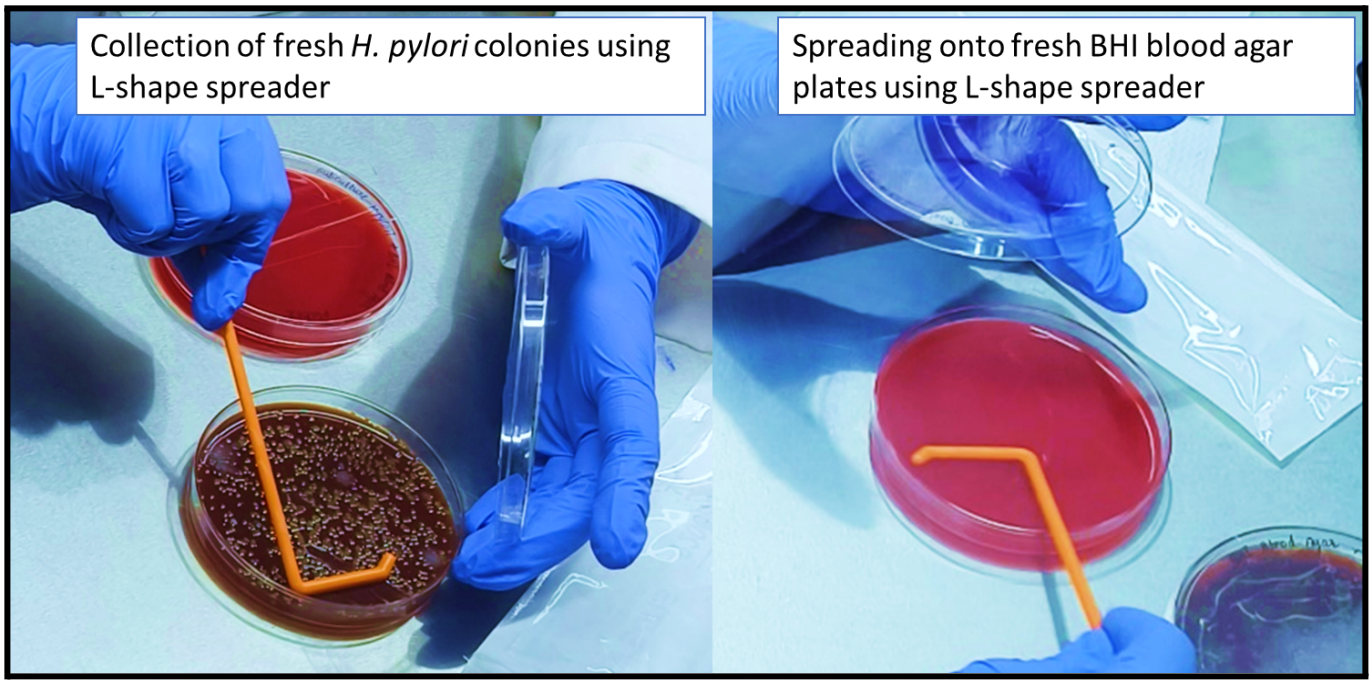

Figure 2: Subculturing procedure of *H. pylori* colonies by spread plate method. Plate full of colonies (left panel) was used to harvest the colonies using a sterile L-shaped disposable spreader and the cells were spread onto the new plate (right panel).

Gastritis is the most common problem all over the world. Especially in countries like India where people ingest a lot of spicy food, gastritis is more frequently observed. In addition to these complications, effects of *Helicobacter pylori* like severe gastritis, gastric ulcers which later on develop as gastric cancer is observed to increase as the years pass by. Nearly 80% of gastric cancers are *H. pylori* related cancers and there is no specific treatment available to *H. pylori* related infections. Though there are some general antibiotics like amoxicillin, tetracycline, ciprofloxacin, Clarithromycin and proton-pump inhibitors were given and they could only control the infections to some extent. To test any drugs or to develop any treatments towards the *H. pylori* the biggest barrier is to culture them. This communication discusses the protocol of how to culture the *H. pylori* in 20 hours of time with the highest efficient colonies for the subcultures from the clinical samples.

H*elicobacter pylori* is a gram negative bacteria which is able to survive in the acidic conditions of the stomach by releasing the urease enzyme to survive and grow in the epithelial cells of gastric walls. Severe gastritis, gastric ulcers, peptic ulcers & gastric cancers are the manifestations that the *H. pylori* can cause. Gastritis is one of the general problems observed world-wide where 6.3 out of every 1,00,000 people were suffering from this problem as of 2020 out of which the range is differing between 2 to 57 in 1,00,000 people for the cases of gastric cancers (1-5). The clinical tests to identify the infection of ulcers and gastritis related to *H. pylori* are Rapid Urease Tests (RUT), ^{13}C Urea Breath Test (^{13}C UBT) (6). The treatments of *H. pylori* are Proton-pump Inhibitors and the general other antibiotics like Clarithromycin, amoxicillin etc., (2,6). Culturing the *H. pylori* is observed to be a task in the general laboratory methods and requires a lot of keen observations, sterility maintenance as there are theories stating that getting the colonies of *H. pylori* takes nearly 72 hours of time or it is generally stated as 3-7 days at 37℃ in the CO_2 incubator as they require microaerophilic conditions for proper growth (6-8). Other requirements besides CO_2 incubator are the maintenance of 2%-5% O_2, 0%-10% of H_2 and also some hydration (2, 9-13). The complications in the culturing of the *H. pylori* is observed when the bacteria is stored even for a day. The efficiency of the *H. pylori* is observed to be high when the biopsy of the infected area is plated in less than three hours in the procedure that we followed at TCABS-E Laboratory. The biopsy of the *H. pylori* infected antrum is directly collected into the Brain-Heart infusion (BHI) broth (purchased from HiMedia Laboratories) and stored on the ice. This stored biopsy is then further homogenized within 30 minutes after collecting the biopsy sample. The homogenization was performed using the basic laboratory

procedures by using the forceps. The forceps were dipped into the 70% isopropanol and placed inside the laminar air flow chamber under UV light for 20 minutes. The sterile forceps were used to chop the pieces of infected antrum biopsy into further more fine pieces. The mixture of the broth and the fine pieces of the biopsy were briefly vortexed carefully for 1 minute. Two hundred µl of the homogenized sample is spread on the BHI Blood agar plates (purchased from HiMedia Laboratories) and is stored in a box of 1.6 L capacity with the anaerobic gas pack (purchased from HiMedia Laboratories) and an oxygen detector tablet (purchased from HiMedia Laboratories) in it. The box containing plates is placed in the incubator at 37ºC for 20 hours.

There were silver-gold coloured colonies observed of diameter ~2 mm each (Figure 1). These colonies were then carefully collected using a sterile L-shaped spreader and are spreaded on to the fresh BHI blood agar plates for subculturing and the same procedure of placing in the box 1.6L capacity box with the microaerophilic conditions at 37ºC for 20 hours is followed (Figure 2). Bacterial colonies from both the original biopsy spread plates and the sub cultured plates will further be used for their 16S rRNA sequencing to identify and confirm if there is any species level diversity in the obtained patient biopsy samples. With this established protocol, we are going to further evaluate our newly designed small molecule compound, HelicoTAC© (15) that was previously patented (202141058294).

Acknowledgements: We thank the Superintendent of King George Hospital permitting us to obtain the patient biopsies. We thank The Yedidi Institute of Discovery and Education, Toronto, Canada, for scientific collaborations.

Conflict of interest: The authors declare no conflict of interest in this study. However, this research article is an ongoing project currently at TCABS-E, Visakhapatnam, India.

Author contributions: M.A. performed all the work under the supervision of R.S.Y., the principal investigator who designed the project, trained M.A. in experiments, secured required material for the project, provided laboratory space, facilities needed and wrote/edited the manuscript.

References

1. https://www.wikidoc.org/index.php/Gastritis_epidemiology_and_demographics#:~:text=The%20prevalence%20of%20eosinophilic%20gastritis%20is%20approximately%206.3%20per%20100%2C000%20individuals%20worldwide.,-Age
2. Thirumurthi, S., & Graham, D. Y. (2012). Helicobacter pylori infection in India from a western perspective. *The Indian journal of medical research*, *136*(4), 549–562.
3. Graham DY, Lu H, Yamaoka Y. African, Asian or Indian enigma, the East Asian *Helicobacter pylori*: facts or medical myths. *J Dig Dis.* 2009;10:77–84.
4. Dikshit RP, Mathur G, Mhatre S, Yeole BB. Epidemiological review of gastric cancer in India. *Indian J Med Paediatr Oncol.* 2011;32:3–11.
5. Tovey FI. *Helicobacter pylori* infection and upper gastrointestinal pathology in a British immigrant Indian community. *Eur J Gastroenterol Hepatol.* 1997;9:647–8.
6. Patel, S. K., Pratap, C. B., Jain, A. K., Gulati, A. K., & Nath, G. (2014). Diagnosis of Helicobacter pylori: what should be the gold standard?. *World journal of gastroenterology*, *20*(36), 12847–12859. https://doi.org/10.3748/wjg.v20.i36.12847.
7. Rojas-Rengifo, D. F., Mendoza, B., Jaramillo, C., Rodríguez-Urrego, P. A., Vera-Chamorro, J. F., Alvarez, J., … Jimenez-Soto, L. F. (2019). Helicobacter pylori culture as a key tool for diagnosis in Colombia. *The Journal of Infection in Developing Countries*, *13*(08), 720–726. https://doi.org/10.3855/jidc.10720.
8. https://www.emro.who.int/emhj-volume-14-2008/volume-14-issue-2/article3.html.
9. Andersen L. P., Nørgaard A., Holck S., Blom J., Elsborg L. Isolation of a "*Helicobacter heilmannii*"-like organism from the human stomach. Eur. J. Clin. Microbiol. Infect. Dis. 1996;15:95–96.
10. Nederskov-Sørensen P., Bjørneklett A., Fausa O., Bukholm G., Aase S., Jantzen E. *Campylobacter pylori* infection and its relation to chronic gastritis. An endoscopic, bacteriologic, and histomorphologic study. Scand. J. Gastroenterol. 1988;23:867–874.
11. Andersen L. P., Elsborg L., Justesen T. *Campylobacter pylori* in peptic ulcer disease: II. Endoscopic findings and cultivation of *C. pylori*. Scand. J. Gastroenterol. 1988;23:760–764.
12. Andersen L. P., Holck S., Povlsen C. O., Elsborg L., Justesen T. *Campylobacter pyloridis* in peptic ulcer disease: I. Gastric and duodenal infections caused by *C. pyloridis*. Histopathologic and microbiologic findings. Scand. J. Gastroenterol. 1987;22:219–224.
13. Nichols L., Sughayer M., DeGirolami P. C., Baloch K., Pleskow D., Eichelberger K., Santos M. Evaluation of diagnostic methods for *Helicobacter pylori* gastritis. Am. J. Pathol.
14. Michael Buenor Adinortey, Charles Ansah, Cynthia Ayefoumi Adinortey, Ansumana Sandy Bockarie, Martin Tangnaa Morna, Damian H. Amewowor, "Isolation of *Helicobacter pylori* from Gastric Biopsy of Dyspeptic Patients in Ghana and *In Vitro* Preliminary Assessment of the Effect of *Dissotis rotundifolia* Extract on Its Growth", *Journal of Tropical Medicine*, vol. 2018, Article ID 8071081, 6 pages, 2018. https://doi.org/10.1155/2018/8071081.
15. Aggunna, M. and Yedidi, R.S. (2022). HelicoTAC©, a PROTAC-based small molecule targeting the virulence factor Cag A of H. pylori as a potential therapeutic for gastritis and gastric cancers. *TCABSE-J*, Vol. 1, Issue 3:46-48. Epub: Oct 5th, 2022.

TCABSE-J Research Article
ISSN: 2583- 2557, *Volume 1, Issue 6, pp4-8. 2023.*

TCABSE-J
Interdisciplinary Sciences Journal

Proton NMR-based comparative analysis of aqueous vs. organic extractions from *Ficus religiosa* leaf with potential applications in the treatment of polycystic ovarian syndrome

Lalithadevi Karri[1, 2], Manikanta Sodasani[1], Santhinissi Addala[1, 3], Abhinav V. K. S. Grandhi[1, 4], Jahnavi Chintalapati[1, 3] and Ravikiran S. Yedidi[1, 5, *]

[1]Department of Intramural research core, The Center for Advanced-Applied Biological Sciences & Entrepreneurship (TCABS-E), Visakhapatnam 530016, A.P. India; [2]Department of Botany, Andhra University, Visakhapatnam 530003, A.P. India; [3]Department of Biochemistry, Andhra University, Visakhapatnam 530003, A.P. India; [4]Koringa College of Pharmacy, Korangi 533461, A. P. India; [5]Department of Zoology, Andhra University, Visakhapatnam 530003, A.P. India. (*Correspondence to R.S.Y.: tcabse.india@gmail.com).

Keywords: PCOS, *F. religiosa*, proton NMR, solvent extraction, aqueous extracts, goat liver extracts, cytochrome P450.

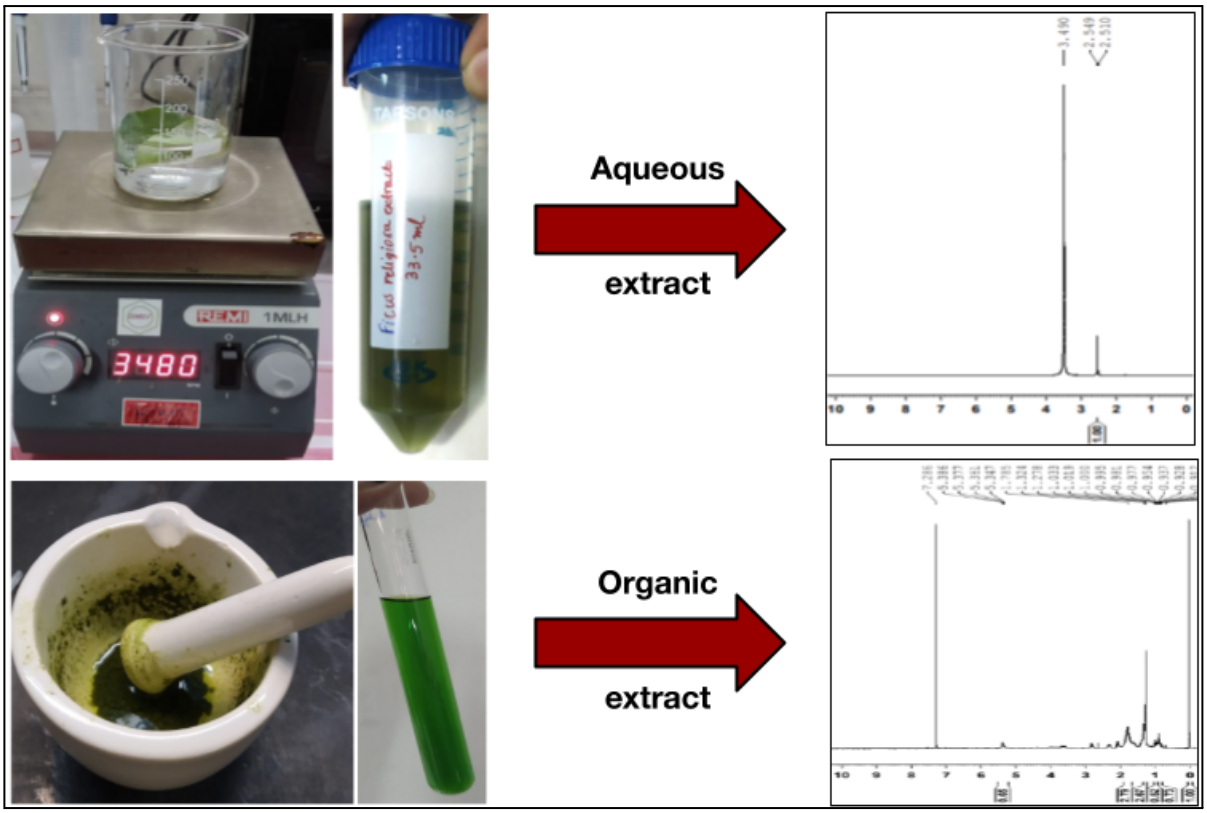

Graphical abstract: Overview of the current study is outlined in this graphical abstract.

Citation: Karri, L., Sodasani, M., Addala, S., Grandhi, A.V.K.S., Chintalapati, J. and Yedidi, R.S. (2023). Proton-NMR-based comparative analysis of aqueous vs. organic extractions from Ficus religiosa with potential applications in the treatment of polycystic ovarian syndrome. *TCABSE-J*, Vol. 1, Issue 6:4-8. Epub: Aug 15th, 2023.

TCABSE-J Research Article

ISSN: 2583- 2557, *Volume 1, Issue 6, pp4-8. 2023.*

TCABSE-J Interdisciplinary Sciences Journal

Polycystic ovarian syndrome (PCOS) prevalence has tremendously increased in recent years in India. Many women in their early teens are facing PCOS issues primarily due to the stress that they go through. Diabetes, obesity, etc. are a few co-morbidities that are commonly observed in PCOS women along with the upregulated secondary sexual characteristics such as facial hair, etc. Recently it has been proposed that the boiled leaf aqueous extracts of *Ficus religiosa* exhibit therapeutic effects on PCOS. In order to understand the importance of the aqueous extracts, we obtained boiled *F. religiosa* leaf aqueous extract and analyzed it using proton-NMR spectrum. In parallel, a methanolic extract of the same was also prepared. The proton NMR spectra of both aqueous and organic extracts were compared. Significant difference was seen in both spectra, as expected, indicating that the extraction method influences the final NMR profile of the sample suggesting that the active ingredients are to be naturally extracted by boiling rather than using the harsh organic solvents. Further phytochemical characterization is currently ongoing to delineate the possible anti-PCOS therapeutic effects of *F. religiosa.*

***F**icus religiosa* is a native fig and considered as sacred plant in India. Under the order Utricales, it belongs to Moraceae, also known as the Mulberry family consisting of diverse trees, shrubs, vines, epiphytes, hemiphytes and rarely herbs [1]. *F. religiosa* is commonly called as peepal tree, bodhi tree in English, Ashvattha tree in India/Nepal or Asathu in Sinhala. This tree is considered as a sacred tree by Hindus, Jains and Buddists [2]. This species is named so because of its religious importance and this is considered as the tree under which Gautam Bhudda was enlightened [2]. Generally *F. religiosa* starts its life cycle as an epiphyte and can live up to 3000 years [1] and has aerial roots which later become vestigial after it starts growing on land. According to the Global Compendium of Weeds this species is listed as "Environmental weed/naturalized weed". This can grow in various climatic conditions and can survive better in tropical rainforests. The only wasp species that pollinate *F. religiosa* is *Blastophaga quadriceps* [1]. This tree is not only treated as sacred due to religious beliefs in India but also due to several medicinal values such as antioxidants in the leaves of peepal trees [3]. Thus, all of its parts viz. leaves, bark, fruits, roots etc. have a lot of importance in the Indian Ayurvedic medicine that has been followed for ages. It is used to treat several disorders related to the central nervous system, endocrine system, gastrointestinal problems, reproductive disorders and some other infectious diseases [4]. It is also believed to have antibacterial, anthelmintic, antioxidant, immunomodulatory, anticonvulsant, hypolipidemic, hypoglycemic and wound healing activities [5-10].

In particular, *F. religiosa* is used in treating reproductive disorders including polycystic ovarian syndrome (PCOS), menorrhagia, infertility in females etc. in the Indian Ayurvedic medicine [11]. Freshly boiled leaf extracts of *F. religiosa* have been used in Ayurveda for PCOS treatment. It has been previously reported that the 3-acetoxy-3-hydroxy propanoic acid (AHPA) in the fresh leaf extracts of *F. religiosa* may have therapeutic effects on PCOS in rats [11]. However, it is not clearly known whether the AHPA has a direct effect on controlling PCOS or its metabolites produced by various CYPs present in the liver during AHPA metabolism that may possess the therapeutic effects.

In this study we performed a comparative analysis of aqueous and organic extract from *F. religiosa* leaf using proton NMR spectra. The leaf was boiled in water and the water was taken as aqueous extract. In order to obtain the organic extract, the lead was homogenized in a mortar and pestle in the presence of methanol.

Materials & Methods:

Collection of F. religiosa leaves: By studying the morphological characteristics of *F. religiosa*, fresh young leaves are collected from the garden of the Botany department of Andhra University.

Preparation of Boiled leaf extract of F. religiosa leaves: This was performed systematically as described below: Day 1: Collected *F. religiosa* leaf is sterilized properly using deionized (di)-water. This leaf is then soaked overnight in a beaker with 100 ml di-water. Day 2: The overnight soaked leaf is then boiled on a hot plate till the water reduces to half. The extract obtained is about 33.5 ml which is left to dry on a plate placed on a hot plate at lowest temperatures till the water has evaporated. We use lower temperatures for the water to evaporate because higher temperatures may affect the constituents present in the extract. The plate with residue of the extract is carefully covered and then placed aside to cool and then this is used for NMR spectroscopy.

Preparation of organic extract of F. religiosa: A fresh young leaf of *F. religiosa* is collected and that is surface sterilized using di-water. This leaf is crushed using mortar and pestle by adding methanol drop by drop till the leaf is completely crushed. Now this extract is filtered using whatmann's filter paper and the filtrate is collected in the test tube. This extract is now left for air drying in the boiling water.

Solubility test of the leaf extracts residue: The dried residue after evaporating the di-water is tested for solubility before NMR spectroscopy. Small amount of the residue is scraped with spatula and a small portion of it is dissolved in dimethyl sulphoxide (DMSO) and another small portion is dissolved in chloroform ($CHCl_3$).

TCABSE-J Research Article
ISSN: 2583- 2557, *Volume 1, Issue 6, pp4-8. 2023.*

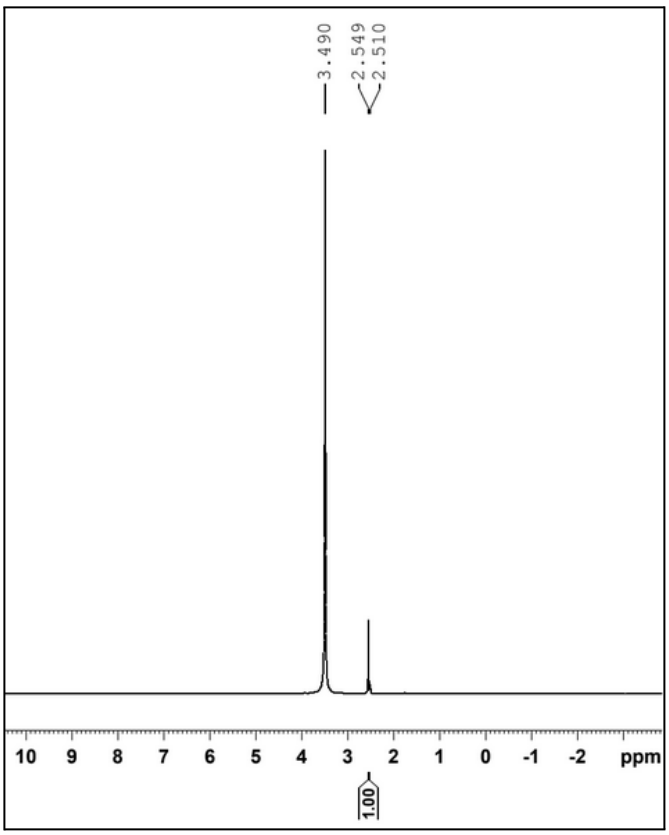

Figure 1. [1]H-NMR spectrum of aqueous extract.

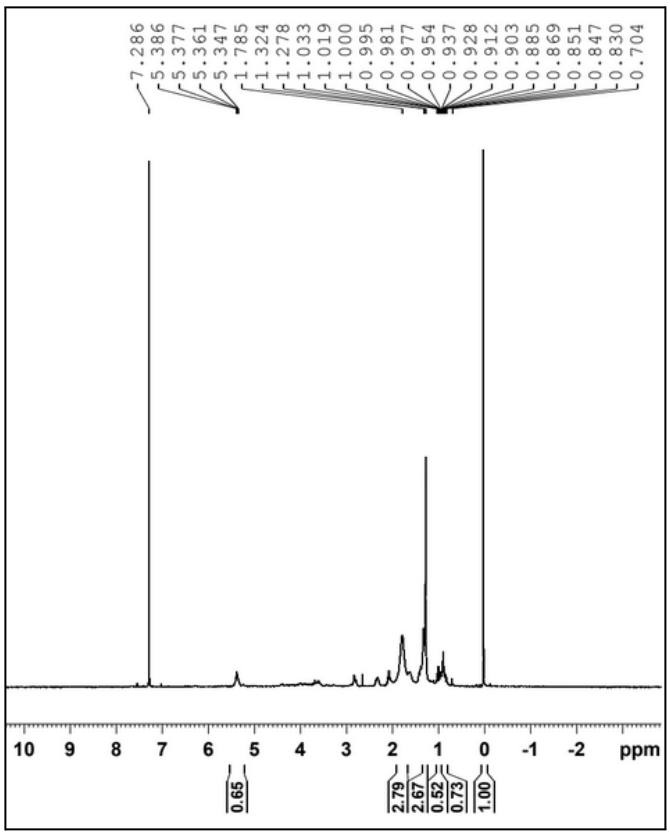

Figure 2. [1]H-NMR spectrum of organic extract.

The residue is completely soluble in DMSO but not in $CHCl_3$. We tested for solubility to decide the heavy solvent used for NMR spectroscopy. Similarly, the solubility of the dried residue from organic solvent was also tested for solubility with DMSO and $CHCl_3$ and found to be soluble in $CHCl_3$.

NMR Spectroscopy: NMR spectroscopy was performed as described previously [12]. Briefly, BRUKER Ascend 400 MHz magnet was used for the acquisition of [1]H-NMR spectra for both samples. The FIDs were deconvoluted and fourier transformed into the individual spectra using TopSpin software. The final spectra are shown in Figures 1 and 2.

Results and Discussion:

Proton NMR spectrum of aqueous extract contains only a few peaks: The proton NMR spectrum of aqueous extract, as shown in Figure 1, contains only three peaks at 3.49 ppm, 2.549 ppm and 2.510 ppm. These peaks are all in the aliphatic region suggesting the absence of any aromatic compounds containing benzene rings specifically. Previously AHPA was reported within *F. religiosa* aqueous leaf extracts.

However, the proton NMR spectrum shown in Figure 1 does not perfectly match AHPA predicted spectrum (Figure 3) from the NMRDB [13-15]. It is noteworthy that the aqueous extract was slightly warmed to dry so that it can be dissolved in heavy solvent for NMR analysis and this warming may cause changes in the AHPA, if at all it was present in the aqueous extract.

The proton NMR spectra show different profiles as expected: The two proton NMR spectra shown in Figures 1 and 2 show different profiles in the context of number of peaks and their positions (ppm) as expected. Normal boiling of the leaf in di-water may only selectively extract the ingredients that are hydrophilic and are easy to extract without damaging the leaf. This may include compounds (may or may not be volatile) that are naturally secreted or exuded by the leaf. Although the AHPA is completely water soluble, comparative analysis of Figures 1 and 3 suggest that the active ingredient that is extracted simply by boiling the leaf in di-water is not AHPA. However, the peaks obtained in Figure 1 are in the aliphatic region suggesting that they could be closely related analogs of AHPA. Along these lines, as shown in Figure 2, the multiple peaks obtained in the organic

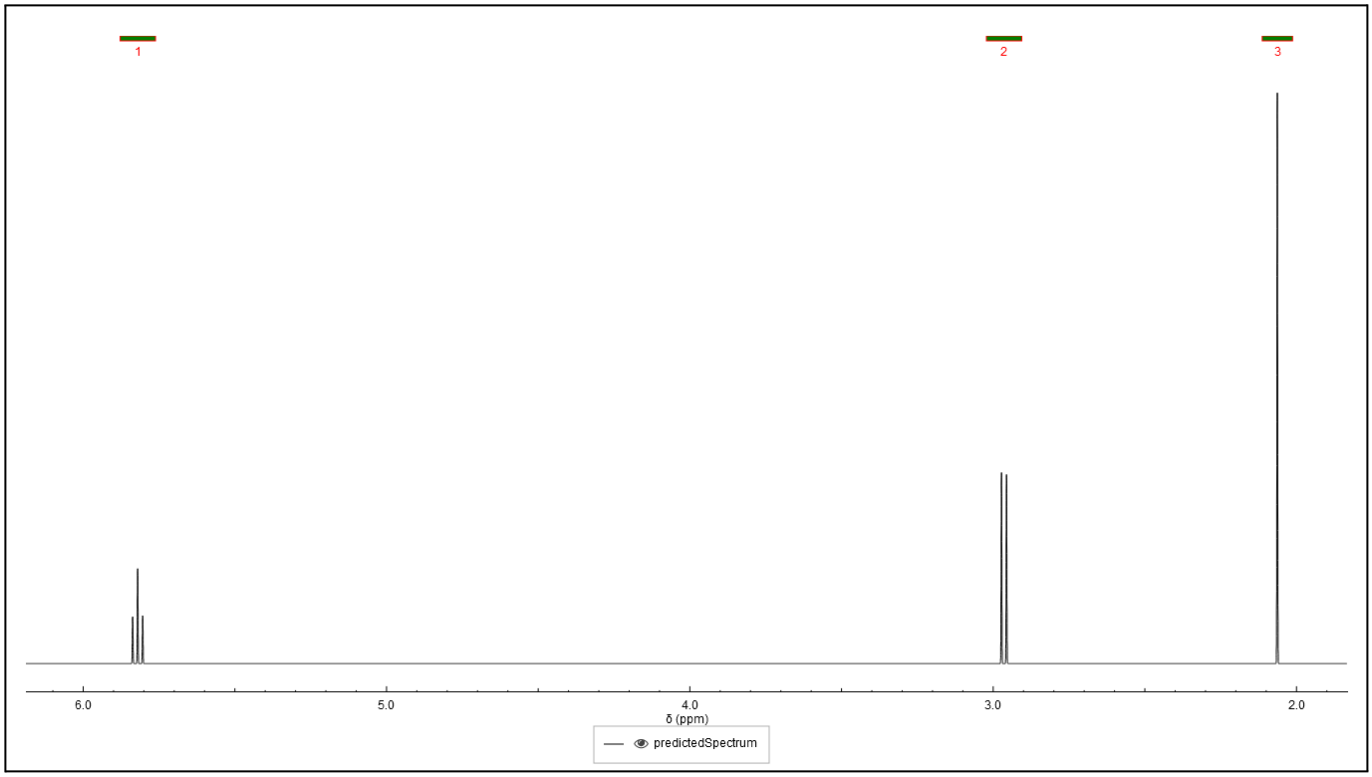

Figure 3. Predicted ^{1}H-NMR spectrum of AHPA.

solvent extract are mostly populated in the aliphatic region suggesting the closely related analogs of AHPA might be present in this extract.

Conclusion and Future directions:

The current study confirms that the AHPA that is believed to be the active ingredient in boiled leaf extract of *F. religiosa* that has anti-PCOS activity is absent based on the proton NMR spectrum. However, this does not conclude the complete absence of AHPA in *F. religiosa*. Maybe the extraction method is not just simply boiling the leaf in water.

Acknowledgements: We thank The Yedidi Institute of Discovery and Education, Toronto for scientific collaborations.

Conflict of interest: The authors declare no conflict of interest in this study. However, this research article is an ongoing project currently at TCABS-E, Visakhapatnam, India.

Author contributions: L.K. collected leaves, prepared aqueous and organic extracts, prepared NMR samples. M.S. and S.A. assisted L.K. in preparation of extracts and solubility tests. A.G. and J.C. assisted L.K. in preparation of NMR samples, data acquisition and analysis. R.S.Y. is the principal investigator who designed the project, trained L.K., M.S., S.A., A.G. and J.C., secured required material for the project, provided the laboratory space and facilities needed, wrote and edited the final version of the manuscript.

References

1. Datil, M. J. and Acevedo-Rodríguez, P. (2022) 'Ficus religiosa (sacred fig tree)', CABI Compendium. CABI International. doi: 10.1079/cabicompendium.24168.
2. Gopukumar, S.; Praseetha, P. Ficus benghalensis Linn–the sacred Indian medicinal tree with potent pharmacological remedies. Int. J. Pharm. Sci. Rev. Res. 2015, 32, 223–227.
3. Murugesu, S., Selamat, J., & Perumal, V. (2021). Phytochemistry, Pharmacological Properties, and Recent Applications of Ficus benghalensis and Ficus religiosa. Plants (Basel, Switzerland), 10(12), 2749. https://doi.org/10.3390/plants10122749.
4. Singh, D., Singh, B., & Goel, R. K. (2011). Traditional uses, phytochemistry and pharmacology of Ficus religiosa: a review. Journal of ethnopharmacology, 134(3), 565–583. https://doi.org/10.1016/j.jep.2011.01.046.
5. Chandrasekar SB, Bhanumathy M, Pawar AT, Somasundaram T. Phytopharmacology of Ficus religiosa. Pharmacogn Rev. 2010 Jul;4(8):195-9. doi: 10.4103/0973-7847.70918. PMID: 22228961; PMCID: PMC3249921.
6. Deepa, P., Sowndhararajan, K., Kim, S., & Park, S. J. (2018). A role of Ficus species in the management of diabetes mellitus:

A review. Journal of ethnopharmacology, 215, 210–232. https://doi.org/10.1016/j.jep.2017.12.045.
7. Gulecha, V., Sivakumar, T., Upaganlawar, A., Mahajan, M., & Upasani, C. (2011). Screening of Ficus religiosa leaves fractions for analgesic and anti-inflammatory activities. Indian journal of pharmacology, 43(6), 662–666. https://doi.org/10.4103/0253-7613.89822
8. Gregory, M., Divya, B., Mary, R. A., Viji, M. M., Kalaichelvan, V. K., & Palanivel, V. (2013). Anti-ulcer activity of Ficus religiosa leaf ethanolic extract. Asian Pacific journal of tropical biomedicine, 3(7), 554–556. https://doi.org/10.1016/S2221-1691(13)60112-4.
9. Singh, D., & Goel, R. K. (2009). Anticonvulsant effect of Ficus religiosa: role of serotonergic pathways. Journal of ethnopharmacology, 123(2), 330–334. https://doi.org/10.1016/j.jep.2009.02.042.
10. Pandit, R., Phadke, A., & Jagtap, A. (2010). Antidiabetic effect of Ficus religiosa extract in streptozotocin-induced diabetic rats. Journal of ethnopharmacology, 128(2), 462–466. https://doi.org/10.1016/j.jep.2010.01.025.
11. Suriyakalaa, U., Ramachandran, R., Doulathunnisa, J. A., Aseervatham, S. B., Sankarganesh, D., Kamalakkannan, S., Kadalmani, B., Angayarkanni, J., Akbarsha, M. A., & Achiraman, S. (2021). Upregulation of Cyp19a1 and PPAR-γ in ovarian steroidogenic pathway by Ficus religiosa: A potential cure for polycystic ovary syndrome. Journal of ethnopharmacology, 267, 113540. https://doi.org/10.1016/j.jep.2020.113540.
12. Mukala, N., Aggunna, M., and Yedidi, R.S. (2023). Sequence homology-based identification of paracetamol metabolizing enzymes in chicken liver homogenates for in vitro drug metabolism studies. TCABSE-J, Vol. 1, Issue 5:12-19. Mar 22nd, 2023. Epub: Oct 25th, 2022.
13. Banfi, D., Patiny, L. www.nmrdb.org: Resurrecting and processing NMR spectra on-line *Chimia*, 2008, *62*(4), 280-281.
14. Andrés M. Castillo, Luc Patiny and Julien Wist. Fast and Accurate Algorithm for the Simulation of NMR spectra of Large Spin Systems. *Journal of Magnetic Resonance* 2011.
15. Aires-de-Sousa, M. Hemmer, J. Gasteiger, " Prediction of 1H NMR Chemical Shifts Using Neural Networks", *Analytical Chemistry*, 2002, *74*(1), 80-90.

Full figure legends:

Figure 1. ^{1}H-NMR spectrum of aqueous extract. A total of 3 peaks are seen in this spectrum and none of these peaks match the predicted spectrum of AHPA.

Figure 2. ^{1}H-NMR spectrum of organic extract. Multiple peaks are seen in this spectrum with most of them populated in the aliphatic region.

Figure 3. Predicted ^{1}H-NMR spectrum of AHPA. Peaks are seen at three different ppms. One singlet and one doublet are seen in the aliphatic region while one triplet is seen at 5.8 ppm.

TCABSE-J Research Article
ISSN: 2583- 2557, *Volume 1, Issue 6, pp9-14. 2023.*

TCABSE-J
Interdisciplinary Sciences Journal

Molecular dynamics simulations of cytotoxin-associated gene A coded protein from *Helicobacter pylori* to probe the flexibility of p53 binding pocket for inhibitor design.

Madhumita Aggunna[1], Abhinav V. K. S. Grandhi[1, 2] and Ravikiran S. Yedidi[1, 3, *]

[1]Department of Intramural research core, The Center for Advanced-Applied Biological Sciences & Entrepreneurship (TCABS-E), Visakhapatnam 530016, A.P. India; [2]Koringa College of Pharmacy, Korangi 533461, A. P. India; [3]Department of Zoology, Andhra University, Visakhapatnam 530003, A.P. India.

(*Correspondence to R.S.Y.: tcabse.india@gmail.com).

Keywords: CagA, *H. pylori*, molecular dynamics simulations, inhibitor design.

Antibiotics and proton pump inhibitors are the only options for the treatment of *Helicobacter pylori* infections till date. However, antibiotic-resistance is already reported clinically against some of these regularly used antibiotics. In this context, novel antibiotics that specifically target the *H. pylori* are needed. Clinically, *H. pylori* infections are broadly classified into several types among which, the cytotoxin-associated gene A (CagA)-positive cases are identified as the ones where the bacterium contains CagA virulence protein that helps in hijacking the intracellular signaling cascades of the host gastric epithelial cells. In this study we explored the p53 binding pocket of CagA protein, taken from PDB ID: 4IRV, *in silico*. Our results indicate that the p53 binding pocket of CagA is flexible to potentially fit a diverse set of small molecules that can be used as inhibitors. Over a 10 ns molecular dynamics simulation we noticed multiple conformational changes leading to changes in the architecture of the p53 binding pocket but the pocket was stable without collapsing throughout the MD simulations indicating that this pocket can be targeted for virtual screening of small molecules. Based on our MD simulations, we conclude that the p53 binding pocket of CagA protein can be used for screening potential inhibitors of *H. pylori* infections.

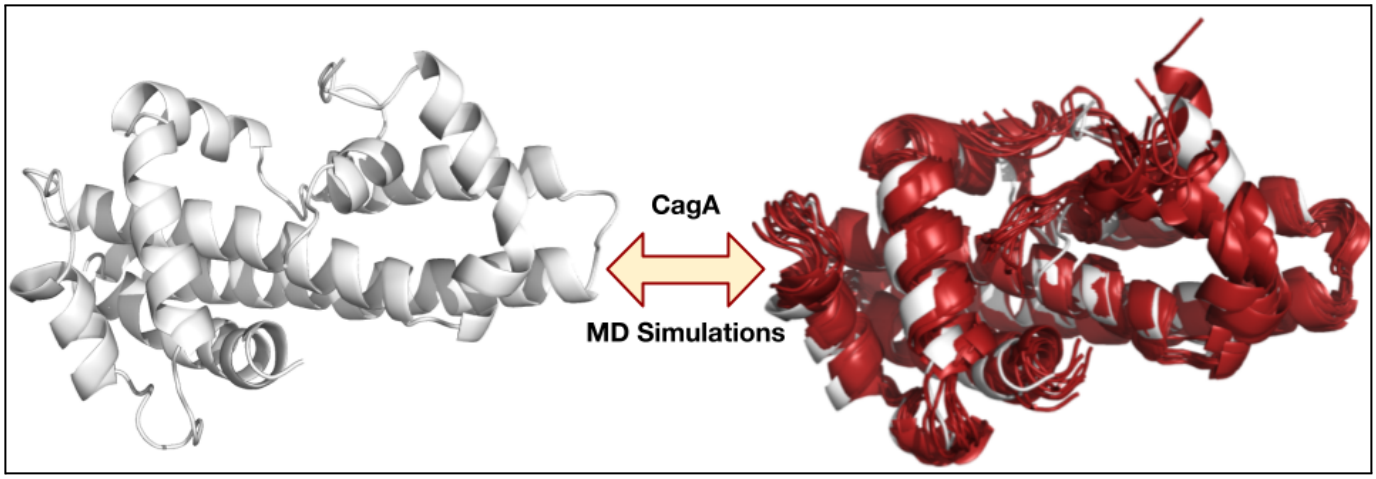

Citation: Aggunna, M., Grandhi, A.V.K.S. and Yedidi, R.S. (2023). Molecular dynamics simulations of cytotoxin-associated gene A coded protein from *Helicobacter pylori* to probe the flexibility of p53 binding pocket for inhibitor design. *TCABSE-J*, Vol. 1, Issue 6:9-14. Epub: Aug 10th, 2023.

TCABSE-J Research Article
ISSN: 2583- 2557, *Volume 1, Issue 6, pp9-14. 2023.*

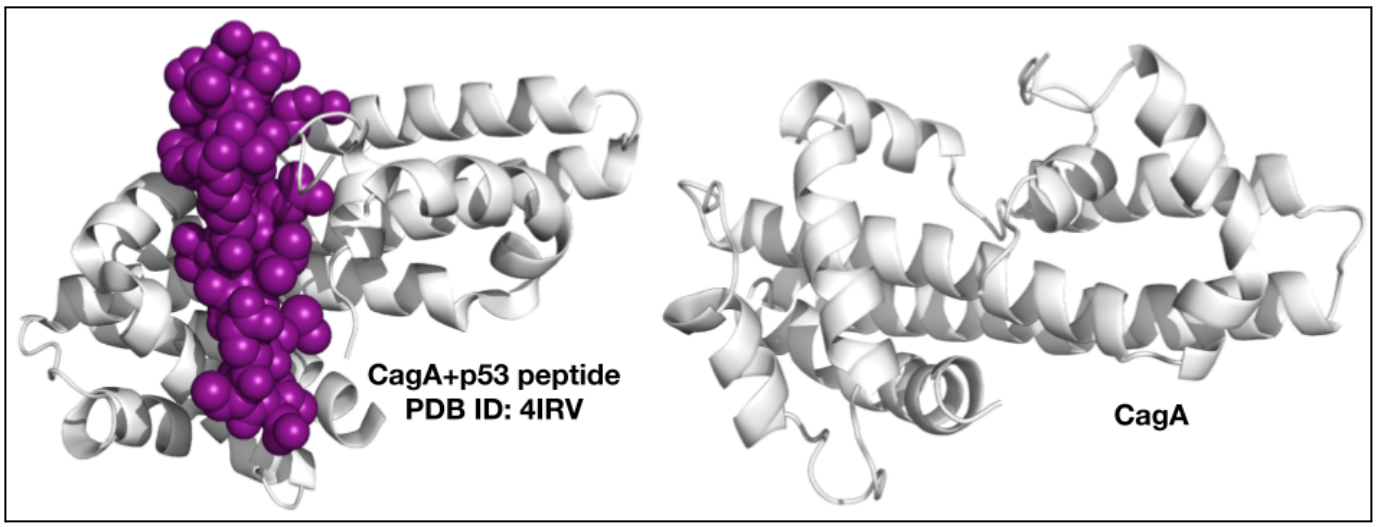

Figure 1. Structures of CagA +/- p53 peptide.

The Cytotoxin Associated gene-A (Cag-A) protein is a virulence factor of the *Helicobacter pylori (H. pylori)* which gets transported to the human gastric cells through the type-4 secretion system (T4SS) by developing a pilus that gets injected to host gastric epithelial cells [1,2,3]. The Cag-A protein coded from the Cag Pathogenic islands, a group of several types of Cag proteins [4,5,6], travels through the pilus. Once the Cag-A protein enters into the human body it participates in the interactions with other host proteins and infects the humans initially as gastritis, then gastric ulcers. The ulcers in the long term cause gastric cancer. The Cag-A protein is an oncogenic protein with a molecular weight between 120 kDa & 140 kDa [6,7,8]. This protein enters the host cell and participates in the downstream signaling by undergoing the kinase phosphorylation dependent and independent. The N-terminal region is kinase phosphorylation independent and inhibits tumor suppressors [6]. The N-terminal region of the Cag-A protein interacts with the Apoptosis stimulating protein of p53-2 protein (ASPP2) and inactivates and degrades the p53 protein [9,10]. The structure of the Cag-A protein is taken further for the molecular dynamic simulations to observe the conformational changes in the binding pocket region [6,11]. The binding pocket of the Cag-A at N-terminus is analyzed to understand the flexibility of the protein which makes the drug design easy. The Cag-A protein is observed to be a protein that is hard to be considered as a drug target and the binding pocket in the N-terminal region that is focused in this paper is also observed to be a long binding pocket which may lead to the complexity for the ligands to bind with low binding affinities. Thus the conformational flexibility of CagA should be explored further.

In this study, the Cag-A structure is taken from the PDB ID: 4IRV (Figure 1) and also the homology model of the same FASTA sequence of the Cag-A [11]. The Cag-A structure and the models were both used for the Molecular Dynamics (MD) simulations using the Desmond Molecular Dynamics System, version 2018-4, D. E. Shaw Research, New York, NY [Schrödinger, LLC, New York, NY].

Materials & Methods:

Preparation of CagA structure: The 3D structure of CagA protein was prepared from the X-ray crystal structure of CagA protein bound to p53 peptide, PDB ID: 4IRV [11]. There were four chains of CagA each bound to one p53 peptide in the structure. Chain A along with the p53 peptide that was bound in the pocket of chain A were kept and the coordinates for the remaining chains were deleted. The final prepared structure file contains one chain of CagA bound to the one chain of p53 peptide. This final file was used further for processing and building the system in order to perform the MD simulations.

CagA homology model building: The FASTA sequence of the Cag-A is taken from the PDB ID: 4IRV and is used to build the 3D homology model of the same using SWISS-MODEL tool (https://swissmodel.expasy.org/) choosing 4IRV as the template sequence. The homology model was built due to main chain breaks in the crystal structure.

Protein pre-processing: CagA protein pre-processing was performed using the Maestro molecular graphics window from Schrödinger LLC, NY. Both CagA from the crystal structure and the CagA homology model were imported into Maestro. Protein preparation wizard was used to pre-process the CagA which includes multiple steps of optimization.

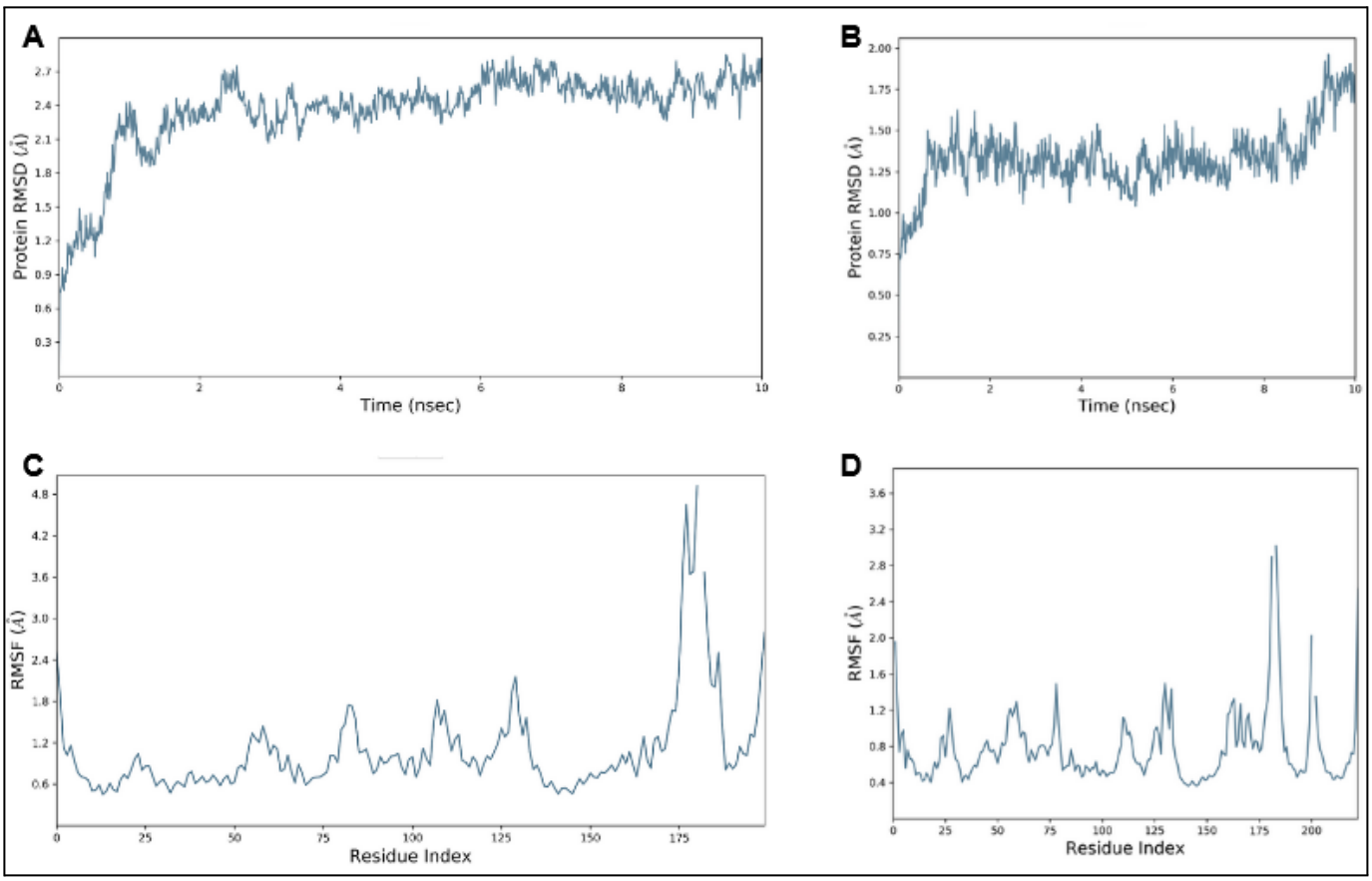

Figure 2. RMSD & RMSF analysis of CagA+/-p53 peptide.

Assignment of bond orders, capping the protein termini, addition of hydrogens, conversion of selenomethionine to methionine and generation of hydrogen bonds. The hydrogen atoms were then optimized by considering the water molecules in the structure. Any close contacts were rectified by relaxing the structure. The processed protein was then used to build the system for MD simulations.

System builder: The processed protein was used to set up the system with periodic boundaries containing the implicit solvent continuum using the SPC water model. The overall volume of the system was minimized by choosing the orthorhombic model. Ions were added and neutralized so that there is no net charge on the system. To mimic the physiological states, 0.15 M salt was added into the system. System builder option of Desmond (D.E. Shaw Research, NY) was used to build the systems for both CagA structure and its homology model.

MD simulations: The MD simulations were performed using Desmond on a 6th generation i5-quad core processor. The system built as described above is loaded into the Maestro molecular graphics window to display all the atoms. Periodic recording of the trajectory at fixed intervals along with the energy was set depending on the total length of the MD simulation. For example, a 10 picoseconds (ps) interval was set for recording the trajectory in order to perform a 10 nanoseconds (ns) MD simulation with an approximate number of 1000 frames per interval. OPLS2005 force field was used to perform the current molecular mechanics-based simulations.

Trajectory analysis: The post MD simulation trajectory was loaded into the Maestro molecular graphics window and was analyzed frame by frame to evaluate any visible structural changes overall and with reference to the p53 binding pocket. The overall protein C_α root mean square deviations (RMSD) and per residue RMS fluctuations (RMSF) were visualized by using the simulation interactions diagram option in Desmond. Both the RMSD and RMSF plots were saved for each MD simulation. Coordinate files at intervals of 1 ns were saved as ".pdb" files to visualize the 3D conformational changes in the protein using Maestro. Figures and movies of the MD simulations were prepared while the trajectory is still loaded into the Maestro molecular graphics window.

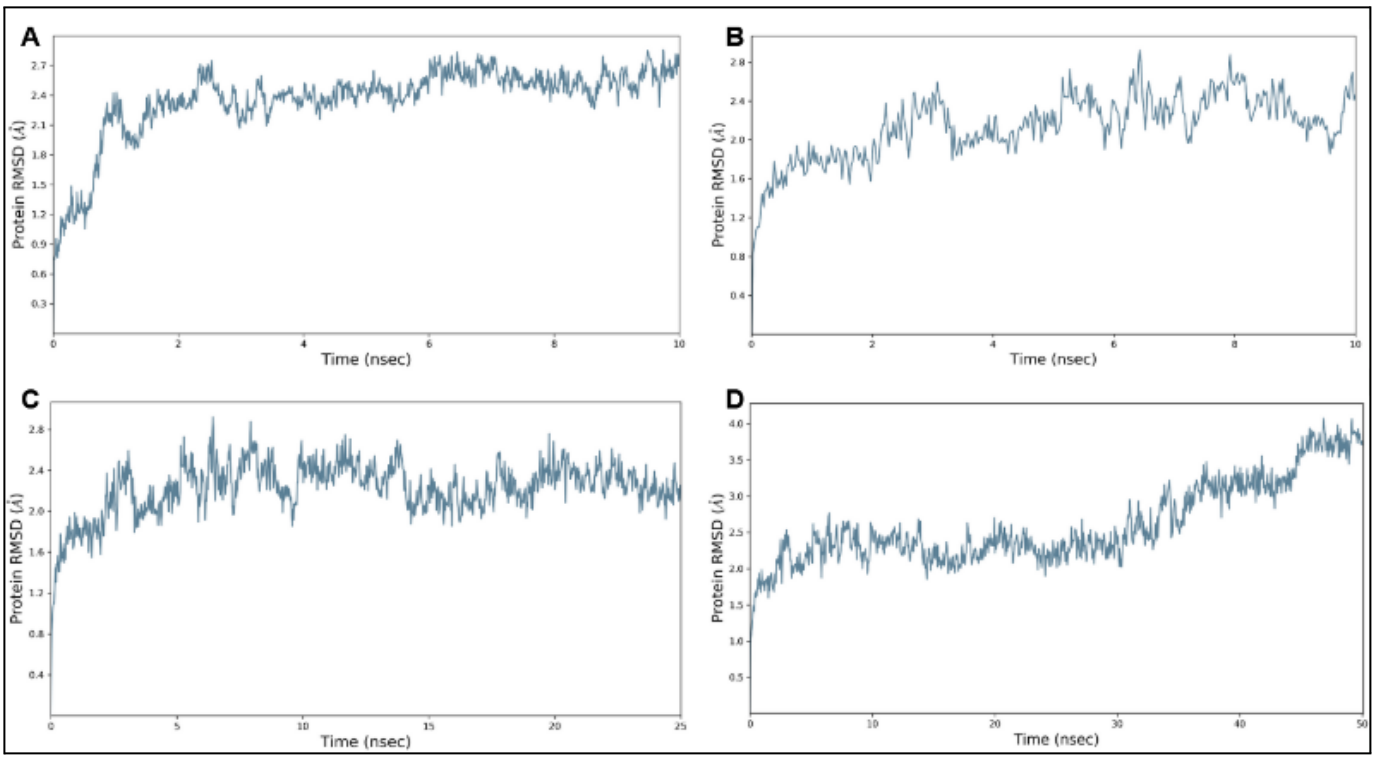

Figure 3. RMSD of CagA structure vs. homology model.

Results and Discussion:

Dimensions of the p53 binding pocket in CagA: The p53 binding pocket in CagA (Figure 1) was roughly measured to be 10 Å in width, 23 Å in length and 10 Å in depth thus adding up a total volume of 2,300 $Å^3$. The p53 peptide in this structure is 20 amino acids long which fits into the above mentioned volume (Figure 1). Such a large binding pocket might be stable with a bigger ligand such as the p53 peptide bound but without a ligand, the stability of such a binding pocket is questionable. In order to delineate this dilemma, we performed 10 ns MD simulations of CagA with and without p53 bound in the pocket.

The protein C_α RMSD of CagA with p53 is slightly lower than without p53: The protein C_α RMSD of CagA, with and without p53 bound, started at 0.75 Å and reached up to 1.6 Å and 2.4 Å at 1 ns, respectively (Figure 2). While the RMSD for CagA with p53 was stable continuously until 8 ns and then increased to 1.75 Å at 10 ns, the RMSD for CagA without p53 increased up to 2.7 Å at 2.5 ns and continued stably until 10 ns. This suggests that the apo protein (CagA without p53) had to go through more RMSD initially compared to the complexed protein. Thus the apo protein exhibited almost 1 Å higher RMSD compared to the p53 bound CagA (Figure 2).

The RMSF profile of apo CagA is different compared to the CagA bound to p53: The overall RMSF for the apo CagA and p53 bound CagA are <2.4 Å and <1.6 Å, respectively, suggesting that the p53 bound CagA has relatively lower RMSF compared to the apo CagA. RMSF values of residue beyond 175 were ignored because of a break in the main chain of the protein in the crystal structure. In order to circumvent this issue, we built a homology model of CagA and used that model for MD simulations.

MD simulations of CagA homology model: The C_α RMSD of CagA homology model is slightly different from the apo CagA that was taken from the crystal structure. As shown in Figure 3, the initial spike at 1 ns that was seen for the apo CagA from the crystal structure was no longer seen in the homology model at 1 ns. Taking this into consideration, we further investigated whether the homology model of CagA will show any major changes in the protein C_α RMSD. So, these MD simulations were further extended to 25 ns and 50 ns (Figure 3). No major spikes were seen within the 25 ns MD simulation. However, the C_α RMSD progressively increased to almost 4 Å from 30 ns to 50 ns in the 50 ns MD simulation.

Higher RMSF is seen in the 50 ns MD simulation compared to the 25 ns MD simulation: The homology model of CagA showed significant changes in the RMSF of its residues when simulated up to 50 ns instead of 25 ns. As shown in Figure 4,

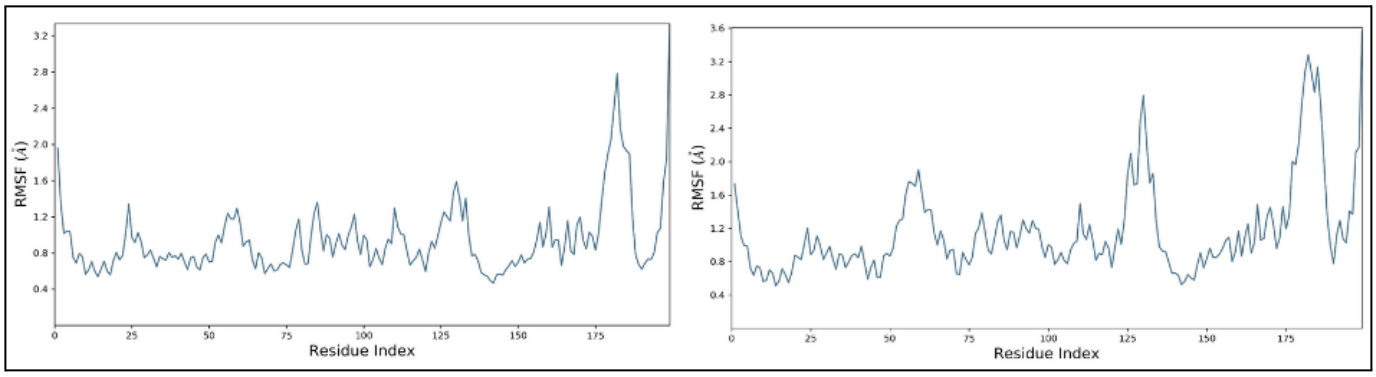

Figure 4. RMSF analysis of CagA homology model.

majorly, three regions were identified where there were significant changes in the RMSF values. These regions are 50-75 (1.2 Å vs. 2.0 Å), 125-150 (1.6 Å vs. 2.8 Å) and 175-185 (2.8 Å vs. 3.2 Å). Comparing Figures 3 and 4, it is safe to say that the residues 125-150 are probably contributing to the unusual behavior of the protein between 30 ns and 50 ns.

Conclusion and Future directions:

The current study clearly demonstrates that the apo CagA possesses more conformational flexibility compared to the p53 bound CagA. Further, the p53 binding pocket showed flexibility in the absence of the ligand suggesting that the volume of this pocket is large and thus, it poses a challenge to screen small molecule leads. We are currently in the process of using the p53 binding pocket of CagA for virtual screening of small molecules with a goal to identify any leads that can be used as potential drugs in the future for the treatment of *H. pylori* infections.

Acknowledgements: We thank The Yedidi Institute of Discovery and Education, Toronto for scientific collaborations.

Conflict of interest: The authors declare no conflict of interest in this study. However, this research article is an ongoing project currently at TCABS-E, Visakhapatnam, India.

Author contributions: M.A. and A.G. performed all the molecular dynamics simulations. R.S.Y. is the principal investigator who designed the project, trained M.A. and A.G., secured required material for the project, provided the laboratory space and facilities needed. M.A., A.G. assisted and R.S.Y. wrote and edited the final version of the manuscript.

References

1. Warren, J. R., & Marshall, B. (1983). Unidentified curved bacilli on gastric epithelium in active chronic gastritis. *Lancet (London, England)*, *1*(8336), 1273–1275.
2. Parsonnet, J., Friedman, G. D., Vandersteen, D. P., Chang, Y., Vogelman, J. H., Orentreich, N., & Sibley, R. K. (1991). Helicobacter pylori infection and the risk of gastric carcinoma. *The New England journal of medicine*, *325*(16), 1127–1131. https://doi.org/10.1056/NEJM199110173251603
3. Forman, D., Newell, D. G., Fullerton, F., Yarnell, J. W., Stacey, A. R., Wald, N., & Sitas, F. (1991). Association between infection with Helicobacter pylori and risk of gastric cancer: evidence from a prospective investigation. *BMJ (Clinical research ed.)*, *302*(6788), 1302–1305. https://doi.org/10.1136/bmj.302.6788.1302
4. Covacci, A., Censini, S., Bugnoli, M., Petracca, R., Burroni, D., Macchia, G., Massone, A., Papini, E., Xiang, Z., & Figura, N. (1993). Molecular characterization of the 128-kDa immunodominant antigen of Helicobacter pylori associated with cytotoxicity and duodenal ulcer. *Proceedings of the National Academy of Sciences of the United States of America*, *90*(12), 5791–5795. https://doi.org/10.1073/pnas.90.12.5791
5. Hatakeyama M. (2017). Structure and function of Helicobacter pylori CagA, the first-identified bacterial protein involved in human cancer. *Proceedings of the Japan Academy. Series B, Physical and biological sciences*, *93*(4), 196–219. https://doi.org/10.2183/pjab.93.013
6. Noto, J. M., & Peek, R. M., Jr (2012). The Helicobacter pylori cag Pathogenicity Island. *Methods in molecular biology (Clifton, N.J.)*, *921*, 41–50. https://doi.org/10.1007/978-1-62703-005-2_7
7. Hatakeyama, M. Oncogenic mechanisms of the *Helicobacter pylori* CagA protein. *Nat Rev Cancer* 4, 688–694 (2004). https://doi.org/10.1038/nrc1433
8. Yong, X., Tang, B., Li, BS. *et al. Helicobacter pylori* virulence factor CagA promotes tumorigenesis of gastric cancer *via* multiple signaling pathways. *Cell Commun Signal* 13, 30 (2015). https://doi.org/10.1186/s12964-015-0111-0
9. Wei, J., Nagy, T. A., Vilgelm, A., Zaika, E., Ogden, S. R., Romero-Gallo, J., Piazuelo, M. B., Correa, P., Washington, M. K., El-Rifai, W., Peek, R. M., & Zaika, A. (2010). Regulation of p53 tumor suppressor by Helicobacter pylori in gastric

epithelial cells. *Gastroenterology*, *139*(4), 1333–1343. https://doi.org/10.1053/j.gastro.2010.06.018

10. Wei, J., Noto, J. M., Zaika, E., Romero-Gallo, J., Piazuelo, M. B., Schneider, B., El-Rifai, W., Correa, P., Peek, R. M., & Zaika, A. I. (2015). Bacterial CagA protein induces degradation of p53 protein in a p14ARF-dependent manner. *Gut*, *64*(7), 1040–1048. https://doi.org/10.1136/gutjnl-2014-307295
11. Nešić, D., Buti, L., Lu, X., & Stebbins, C. E. (2014). Structure of the Helicobacter pylori CagA oncoprotein bound to the human tumor suppressor ASPP2. *Proceedings of the National Academy of Sciences of the United States of America*, *111*(4), 1562–1567. https://doi.org/10.1073/pnas.1320631111

Full Figure Legends:

Figure 1. Structures of CagA +/- p53 peptide. CagA bound to the p53 peptide (purple color spheres) is shown on the left and the CagA after removing the coordinates for p53 peptide (apo CagA) is shown on the right.

Figure 2. RMSD & RMSF analysis of CagA+/-p53 peptide. Panels A and B show the protein C_α RMSD of apo CagA and CagA-p53 complex taken from PDB ID: 4IRV, respectively. Apo CagA shows an initial spike at 1 ns that was not seen in the complex but the complex showed a spike after 8 ns that was absent in the apo CagA protein. Panels C and D show the protein RMSF of apo and complex CagA, respectively. The overall RMSF for the apo CagA and p53 bound CagA are <2.4 Å and <1.6 Å, respectively

Figure 3. RMSD of CagA structure vs. homology model. RMSD of apo CagA from the crystal structure is shown in panel A as a reference. Panel B shows the RMSD of apo CagA homology model in which the initial spike at 1 ns is absent. Panels C and D show 25 ns and 50 ns MD simulations of the homology model. No major spikes were seen within the 25 ns MD simulation. However, there is a spike that progressively increased to almost 4 Å from 30 ns to 50 ns in the 50 ns MD simulation.

Figure 4. RMSF analysis of CagA homology model. The 25 ns and 50 ns MD simulations of the CagA homology model are shown on the left and right, respectively. Three regions: 50-75 (1.2 Å vs. 2.0 Å), 125-150 (1.6 Å vs. 2.8 Å) and 175-185 (2.8 Å vs. 3.2 Å) showed significant changes in the RMSF values.

TCABSE-J Communications
ISSN: 2583- 2557, *Volume 1, Issue 6, pp15-17. 2023.*

In vitro comparative analysis of leaky protein expression in the BL21 strain vs. DH5α strain of *E. coli*.

Manikanta Sodasani[1], Srirajini Bukka[1, 2], Niharikha Mukala[1, 2], Bindiya Panchagnula[2], Sudhakar Pola[2], and Ravikiran S. Yedidi[1, 3, *]

[1]Department of Intramural research core, The Center for Advanced-Applied Biological Sciences & Entrepreneurship (TCABS-E), Visakhapatnam 530016, A.P. India; [2]Department of Biotechnology, Andhra University, Visakhapatnam 530003, A. P. India; [3]Department of Zoology, Andhra University, Visakhapatnam 530003, A. P. India. (*Correspondence to R.S.Y.: tcabse.india@gmail.com).

Keywords: Leaky expression, BL21, DH5-alpha, *E. coli*, protein expression, SDS-PAGE.

Protein expression using the bacterial expression system is routinely used not only in the research laboratories on a small scale but also in the industrial bulk productions. Usually no lethality is posed for the bacterial cells if the protein of interest (POI) is not toxic. However, certain proteins could pose lethality to the bacterial cells due to various reasons. Hence leaky expression of proteins is highly undesirable especially if the POI is toxic to the bacterial cells. In this study, we used a plasmid containing SARS CoV-2 spike protein-receptor binding domain (RBD) to test whether its expression is leaky in 2 different strains of *E. coli* viz. DH5α and BL21. Further, we evaluated any possible lethality posed by the expression of RBD in both strains. Our results suggest that RBD expression was leaky and independent of the T7 promoter that was designed in frame with RBD. Expression of RBD was not lethal to both strains of *E. coli*.

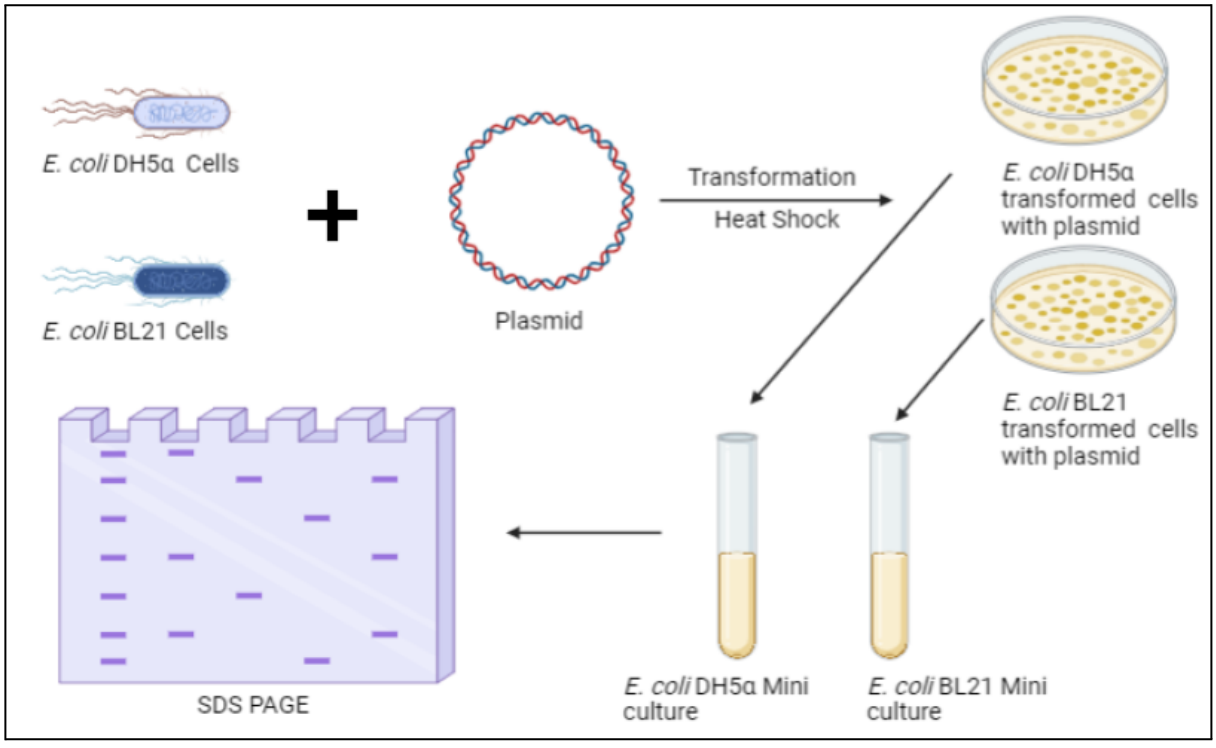

Citation: Sodasani, M., Bukka, S., Mukala, N., Panchagnula, B., Pola, S. and Yedidi, R.S. (2023). *In vitro* comparative analysis of leaky protein expression in the BL21 strain vs. DH5α strain of *E. coli*. *TCABSE-J*, Vol. 1, Issue 6:15-17. Epub: Aug 19th, 2023.

TCABSE-J Communications
ISSN: 2583- 2557, *Volume 1, Issue 6, pp15-17. 2023.*

Figure 1. Colonies of transformants, DH5α (left) and BL21 (right).

Recombinant expression and purification of proteins is in general feasible with some difficulties but the same is not true for the membrane proteins [1]. Various genetic strategies have been explored for proper expression and purification of difficult to express or insoluble proteins [2-4]. The BL21 strain of *E. coli* is prominently used because it has been genetically engineered such that it lacks proteases [5-7]. The strain "B" that lacks the lon protease "L" is the BL21 strain. Lack of proteases implies low degradation of the expressed protein of interest in the BL21 strain. On the other hand, maintenance of expression plasmids is equally important with proper strains of *E. coli* such as the DH5α that have the recA mutation and/or deletion in the genome [8, 9]. In order to ease the protein expression especially for purposes of high throughput nature, various optimizations such as codon optimization, designing disulfide bonds, co-expression of chaperones, high density bacterial cultures, etc. have been successfully tested [10-15]. Irrespective of the toxicity of the expressed protein, overexpression in combination with solubility issues may lead to the formation of inclusion bodies from which the protein of interest has to be recovered [16-19]. Usually proteins without folding problems can easily be recovered from the inclusion bodies through the denaturation process using chaotropic agents such as urea. In this study, we evaluated the leaky expression of a gene cloned into a protein expression vector using the *E. coli* DH5α and BL21 strains. Both strains were cultured with the plasmid and the whole cell extracts were used to run the SDS-PAGE for the detection of protein expression.

Materials & Methods:

Transformation of E. coli cell with plasmid: Both strains of *E. coli*, DH5α and BL21 were transformed with the plasmid carrying the gene of interest. This plasmid has ampicillin selection with β-lactamase gene along with mCherry tag followed by the gene of interest. Heat-shock method of transformation was used. Fresh vials of both strains each containing 100 µl of competent cells were taken to which 2 µl of plasmid per vial was added and incubated on ice for 30 min. The vials were then kept at 42 ℃ for 30 sec and were immediately placed on ice. One ml of presterilized SOC medium was added to each vial and both vials were incubated at 37 ℃ for 1 hr. Freshly prepared LB agar plates using autoclaved LB agar medium were used for plating the transformants. Post incubation, the transformed cells were plated on LB agar plates containing 30 mcg ampicillin. Plates were incubated at 37 ℃ overnight.

Overnight bacterial minicultures: Freshly prepared LB broth was taken in two culture tubes 5 ml each. One tube was inoculated with the DH5α colonies and the other was inoculated with the BL21 colonies. Both tubes were incubated at 37 ℃ overnight. Fresh LB broth (5 ml per tube) was added to the overnight cultures and the cultures were further incubated for 6 hours before harvesting them.

Cell lysis and sample preparation: Cells were harvested by centrifugation at 5000 rpm for 20 min. Supernatants were discarded safely into a beaker containing bleach or 70% alcohol. The pellets were then resuspended in the residual supernatant. Equal volumes of lysis solution were added to both tubes and the contents were boiled at 95 ℃ for 10 min. After cooling down the samples, they were centrifuged at 14,000 rpm for 15 min. Supernatants were carefully transferred to new tubes to load and run the SDS-PAGE.

SDS-PAGE: The 12% separating gel was first prepared in a centrifuge tube containing 6 ml of 30% acrylamide-bisacrylamide + 6 ml of 2.5X Tris-SDS buffer (pH 8.8) + 10% ammonium persulfate + TEMED + deionized water. The separating gel was poured in between the plates and isopropanol on the top to prevent uneven edges on the top. Once the separating gel is solidified, the 5% stacking gel is prepared in a centrifuge tube containing 1.3 ml of 30% acrylamide-bisacrylamide + 1.6 ml of 5X Tris-SDS buffer (pH 6.8) + 10% ammonium persulfate + TEMED + deionized water. The isopropanol was removed and the stacking gel was poured and the comb was placed on the top. Samples were loaded (15 µl per well) and the gel was run at 120 V. Gel was stained/destained to visualize protein bands.

Results and Discussion:

Multiple colonies were obtained for both DH5α and BL21 transformants: The LB agar plates containing colonies of transformants are shown in Figure 1. Both DH5α and BL21 transformants yielded multiple colonies on the ampicillin plate confirming the presence of the plasmid (transformants). The number of colonies in the case of BL21 plate are visibly countable while the other plate showed a lawn of bacterial colonies suggesting that the transformation was very efficient in both cases.

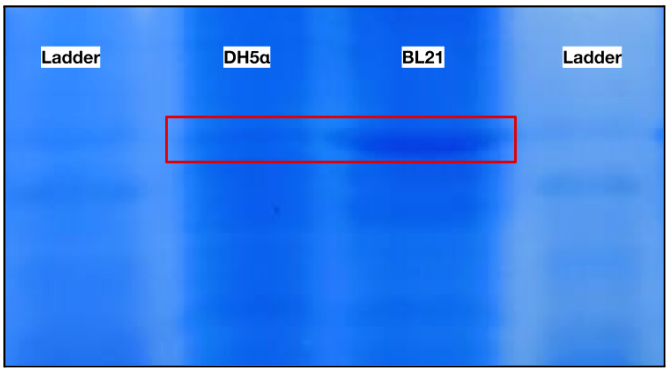

Figure 2. SDS-PAGE analysis of leaky expression.

Leaky expression was seen in both strains on SDS-PAGE: The whole cell extracts of the bacterial cells were analyzed by using SDS-PAGE as shown in Figure 2. Both strains showed the protein expression that is highlighted by the red box in Figure 2. The BL21 strain showed a significantly visible thick band while the other strain gave a faint band that aligned to the same molecular weight. This suggests that both strains were capable of expressing the protein of interest (POI) without inducing the promoter with IPTG. The POI tested here is a non-toxic protein hence, it did not pose any lethality to the bacterial cells. However, if the POI were toxic, then the final yield of POI would have been significantly low due to several reasons such as inefficient growth of the cultures, degradation of the excess POI that was produced, etc. Both bands were quantified using ImageJ software [20]. We found that the pixel-based intensity of the BL21 band is more than 10-fold higher when compared to the DH5α band in the SDS-PAGE. The current study proves that certain plasmids, even though have a promoter that can be externally controlled, there might still be some leaky expression of the POI. However, if the POI is toxic to the cells then the overall yield of the POI will be low thus affecting the final yield of the recombinant protein.

Acknowledgements: We thank The Yedidi Institute of Discovery and Education, Toronto for scientific collaborations. The authors declare no conflict of interest in this study.

References

1. Miroux B, Walker JE. Over-production of proteins in Escherichia coli: mutant hosts that allow synthesis of some membrane proteins and globular proteins at high levels. J Mol Biol. 1996;260:289–298.
2. Sørensen HP, Mortensen KK. Advanced genetic strategies for recombinant protein expression in Escherichia coli. J Biotechnol. 2005;115:113–128.
3. Guleria R, Jain P, Verma M, Mukherjee KJ. Designing next generation recombinant protein expression platforms by modulating the cellular stress response in Escherichia coli. Microb Cell Fact. 2020;19:1–17.
4. Mital S, Christie G, Dikicioglu D. Recombinant expression of insoluble enzymes in Escherichia coli: a systematic review of experimental design and its manufacturing implications. Microb Cell Fact. 2021;20:1–20.
5. Chaudhary AK, Lee EY. Tightly regulated and high level expression vector construction for Escherichia coli BL21(DE3) J Ind Eng Chem. 2015;31:367–373.
6. Chan WT, Verma CS, Lane DP, Gan SK (December 2013). "A comparison & optimization of methods & factors affecting the transformation of Escherichia coli Bioscience Reports. 33 (6).
7. Adrio, J. L., and Demain, A. L. (2010). Recombinant organisms for production of industrial products. Bioeng. Bugs 1, 116–131.
8. Bryant FR (June 1988). "Construction of a recombinase-deficient mutant recA protein that retains single-stranded DNA-dependent ATPase activity". The Journal of Biological Chemistry. 263 (18): 8716–8723.
9. Taylor RG, Walker DC, McInnes RR (April 1993). "E. coli host strains significantly affect the quality of small scale plasmid DNA preparations used for sequencing". Nucleic Acids Research. 21 (7): 1677–1678.
10. Angov, E., Legler, P. M., and Mease, R. M. (2011). Adjustment of codon usage frequencies by codon harmonization improves protein expression and folding. Methods Mol. Biol. 705, 1-13.
11. Bessette, P. H., et al. (1999). Efficient folding of proteins with multiple disulfide bonds in the Escherichia coli cytoplasm. Proc. Natl. Acad. Sci. U.S.A. 96, 13703-13708.
12. Braun, P. and LaBaer, J. (2002). High throughput protein production for functional proteomics. Trends Biotechnol. 21, 383-388.
13. Choi, J. H., Keum, K. C. and Lee, S. Y. (2006). Production of recombinant proteins by high cell density culture of Escherichia coli. Chem. Eng. Sci. 61, 9.
14. Demain, A. and Vaishnav, P. (2009). Production of recombinant proteins by microbes and higher organisms. Biotechnol. Adv. 27, 297-306.
15. de Marco, A. et al. (2007). Chaperone-based procedure to increase yields of soluble recombinant proteins produced in E. coli. BMC Biotechnol. 7:32.
16. Dumon-Seignovert, L., Cariot, G. and Vuillard, L. (2004). The toxicity of recombinant proteins in Escherichia coli: a comparison of overexpression in BL21(DE3), C41(DE3) and C43(DE3). Protein Expr. Purif. 37, 203-206.
17. Gonzalez-Montalban, N., Garcia-Fruitos, E., and Villaverde, A. (2007). Recombinant protein solubility - does more mean better? Nat. Biotechnol. 25, 718–720.
18. Thomas J.G., Baneyx F. Protein misfolding and inclusion body formation in recombinant Escherichia coli cells overexpressing Heat-shock proteins. J. Biol. Chem. 1996;271:11141–11147.
19. Blackwell J.R., Horgan R. A novel strategy for production of a highly expressed recombinant protein in an active form. FEBS Lett. 1991;295:10–12.
20. Posimsetti, M., Sanapala, S. S., Vissapragada, M. and Yedidi, R. S. (2022). Design of a pixel-based quantification method for in vitro colorimetric enzyme assay to evaluate enzyme inhibition in a dose-dependent manner. TCABSE-J, Vol. 1, Issue 4:22-27. Epub: Oct5th, 2022.

TCABSE-J Research Article
ISSN: 2583- 2557, *Volume 1, Issue 6, pp18-23. 2023.*

PCR-amplification of wild type receptor binding domain coding gene of SARS CoV-2 spike protein for cloning into a bacterial expression vector

Madhuri Vissapragada[1], Suvarna Gollu[1,2], Santhinissi Addala[1], Manikanta Sodasani[1], Madhumita Aggunna[1], Niharikha Mukala[1, 2], Bindiya Panchagnula[2], Sudhakar Pola[2] and Ravikiran S. Yedidi[1, 3, *]

[1]Department of Intramural research core, The Center for Advanced-Applied Biological Sciences & Entrepreneurship (TCABS-E), Visakhapatnam 530003, A.P. India; [2]Department of Biotechnology, Andhra University, Visakhapatnam 530003, A. P. India; [3]Department of Zoology, Andhra University, Visakhapatnam 530003, A. P. India. (*Correspondence to R.S.Y.: tcabse.india@gmail.com).

Keywords: SARS CoV-2, Spike protein, receptor binding domain, PCR, primer design, agarose gel electrophoresis.

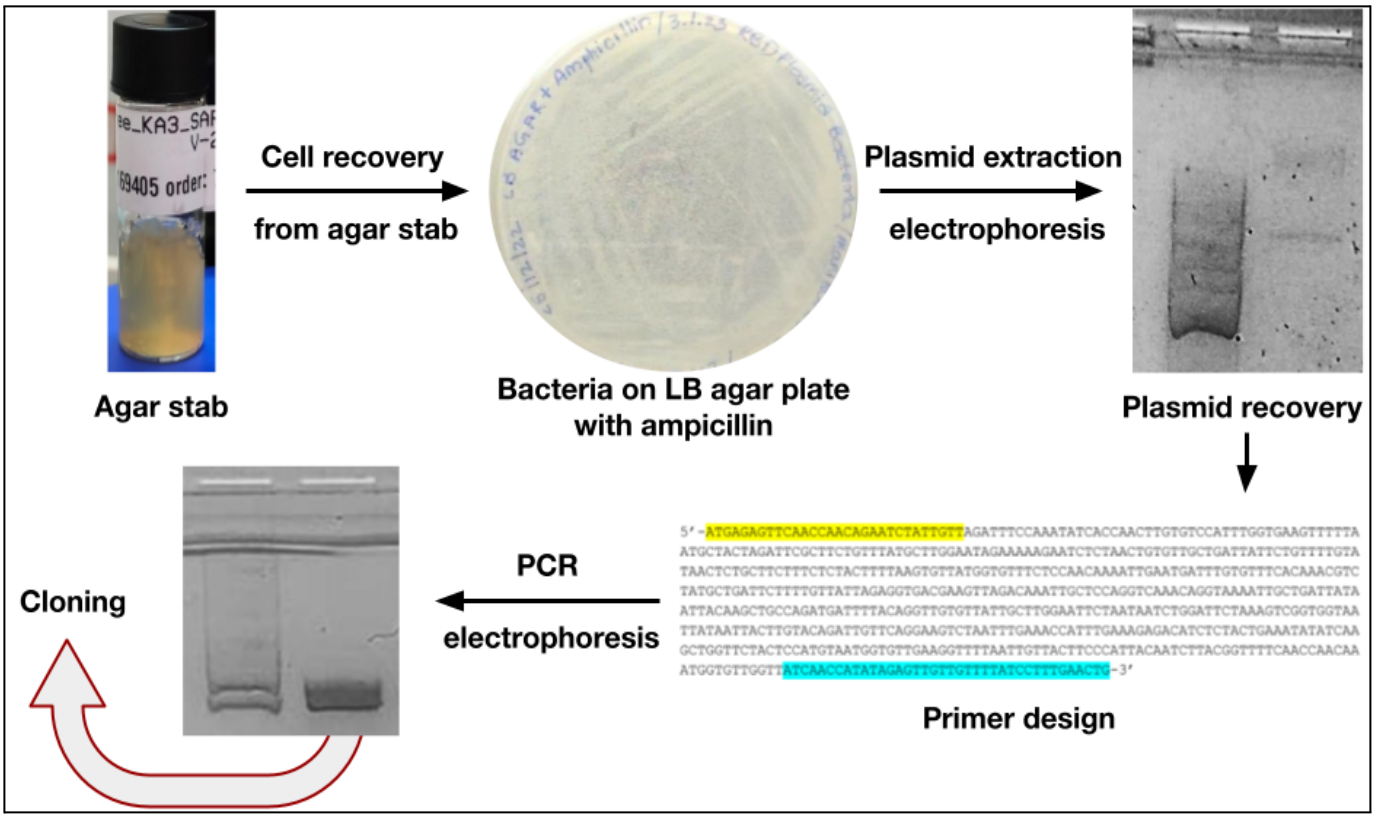

Graphical abstract outlining the overall process of this study.

Citation: Vissapragada, M., Gollu, S., Addala, S., Sodasani, M., Aggunna, M., Mukala, N., Pola, S., Panchagnula, B. and Yedidi, R.S. (2023). PCR amplification of wild type receptor binding domain coding gene of SARS CoV-2 spike protein for cloning into a bacterial expression vector. *TCABSE-J*, Vol. 1, Issue 6:18-23. Epub: Aug 20th, 2023.

TCABSE-J Research Article
ISSN: 2583- 2557, *Volume 1, Issue 6, pp18-23. 2023.*

PCR-based amplification of genes is routinely done these days due to the availability of new varieties of DNA polymerases with high fidelity. COVID-19 is a pandemic that has claimed millions of lives across the globe in recent years. Vaccines were designed and were employed in time as a rescue mechanism. However, the viral evolution through mutations in its spike protein is out competing the vaccine design strategies that exist today. Newer ways are needed for vaccine design. In this study, we PCR-amplified the SARS CoV-2 spike protein receptor binding domain (RBD) using specific primers. The PCR product size was confirmed using agarose gel electrophoresis. The annealing temperatures were thoroughly scanned to identify the best one. This PCR product shows the correct size on the gel compared to the standard 1kb DNA ladder. In future, this PCR product will be cloned into an expression vector (pET) in order to express and evaluate the protein for a better vaccine design.

COVID-19, a global pandemic, was caused by Severe Acute Respiratory Syndrome Coronavirus 2 (SARS-CoV-2) during 2019 - 2020. SARS-CoV-2 was first reported in Wuhan, China in December 2019. SARS-CoV-2 virus belongs to the coronaviridae family and was found to be closely related to human pathogenic corona viruses like SARS-CoV-1 which caused the 2002 - 2004 outbreak and MERS. Properties like high reproductive number, stronger interaction with the host cells and efficient spreading capacity have turned SARS-CoV-2 a more infectious one compared to the other viruses of the same family [1][2]. Corona virus has four important structural proteins, out of which Spike protein [S] is found to play a major role in the processes of - entry of the viral particle, attachment and fusion of the viral membranes with the host cell membrane [3][4]. Spike protein is a homotrimeric membrane protein having two subunits S1 and S2 in each monomer. RBD is present in the S1 subunit and is of 200 amino acids length [5][6].

The receptor binding domain (RBD) of the spike protein is an important region of the spike protein structure which facilitates the interaction of the spike protein with the human ACE2 receptor. RBD of the spike protein is also an important target for the production of antibodies and in the development of drugs and vaccines [7][8][9]. Hence, RBD has been the major target for therapeutic development based studies on COVID-19 caused by SARS-CoV-2. But in the process of evolution, many variants of SARS-CoV-2 have emerged which pose a challenge for the existing drugs and vaccines working against the RBD in the spike protein of SARS-CoV-2. Owing to the above mentioned necessity, we are in the process of development of newer vaccine strategies for COVID-19 pandemic that aims to target multiple existing and emerging variants of SARS-CoV-2 and to provide safer and less invasive vaccine administration. As the preliminary requirement of the research is the availability of the RBD gene in desired quantities, we believe that the optimization of PCR-based amplification of RBD gene will help to generate multiple copies of the same for further use. In this study, we have focussed on optimization of PCR-based amplification of the receptor binding domain gene from SARS-CoV-2 spike protein in order to use it for cloning purposes.

Materials & Methods:

Bacterial strains and plasmids: Escherichia coli, DH5α strain cells were used in this study. *E. coli*, DH5α strain cells containing the RBD plasmids were purchased from Addgene (#169405) as agar stabs. The SARS-CoV-2 RBD plasmid used for transformation was pmCellFree_KA3_SARS-COV-2_RBD was a gift from Kirill Alexandrov (Addgene plasmid #169405; http://n2t.net/addgene:169405; RRID: Addgene_169405) [10].

Media preparation and bacterial cell culture: Luria Bertani (LB) Broth and LB Agar plates were used for culturing the *E. coli*, DH5α cells. LB Broth was purchased from HiMedia (catalog no. M1245). The liquid broth and agar plates were prepared according to the manufacturer's instructions. One hundred ml of broth was prepared by adding 2.5 grams of LB broth powder to 100 mL of di-water. Similarly for LB Agar plate preparation, to 300 mL of di-water, 7.5 grams of LB Broth powder and 4.5 grams of Agar-Agar (Bacteriological grade) were added. Both the solutions were mixed well and autoclaved at 121 °C temperature and 15 lb pressure for 20 minutes. Ampicillin (final conc. 50 mcg) was added to the nutrient media. LB Agar solution was poured into petri plates and cooled to solidify. The *E. coli* cells containing the RBD plasmid which were obtained as agar stab were initially streaked on LB Agar + Amp plates and incubated at 37 °C overnight (Figure 1). The following day, a loopful of colonies were inoculated into 5 ml of LB Broth with ampicillin and incubated at 37 °C overnight.

S.no	Component	Volume
1	Emerald Amp GT PCR Master Mix (2X Premix) (Takara #RR310)	25 µl
2	DI Water	21 µl
3	RBD Plasmid DNA (Template DNA)	2 µl
4	Forward Primer	1 µl
5	Reverse Primer	1 µl
	Total	50 µl

Table 1. Composition of PCR for 2 µl of template DNA.

TCABSE-J Research Article
ISSN: 2583- 2557, *Volume 1, Issue 6, pp18-23. 2023.*

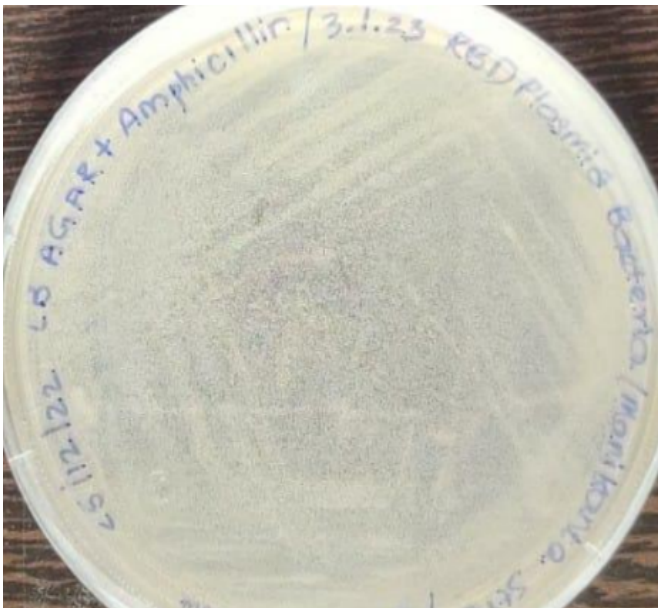

Figure 1. LB agar plate showing cell recovery from agar stab.

Plasmid DNA isolation: The overnight culture which was inoculated with *E. coli* cells containing the RBD plasmid was used to perform plasmid DNA extraction. Plasmid DNA Extraction kit (Column based) purchased from HiMedia (catalog no. MB505) was used to perform plasmid DNA extraction, according to manufacturer's instructions. Cells from the overnight culture were harvested by centrifugation. The culture was centrifuged at 12,000 rpm for 1 min. The culture media was discarded and the pellet containing the bacterial cells was resuspended in 250 µl of resuspension solution containing RNase. The pellet was resuspended without any clumps by mixing thoroughly by pipetting. To the resuspended bacterial cells, 250 µl of Lysis solution was added and mixed gently by inverting the tube 4-5 times. Next, 350 µl of neutralization solution was added and mixed gently by inverting the tube 4-5 times. A cloudy white precipitate was observed after adding the neutralization solution. The cells were centrifuged at 12,000 rpm for 10 minutes. The clear supernatant was transferred to a spin column carefully and centrifuged at 12,000 rpm for 1 minute. The flowthrough was discarded. To the spin column, 500 µl of wash solution (HPB) was added and centrifuged at 12,000 rpm for 1 minute. The flow-through was discarded. To the spin column 700 µl of wash solution containing ethanol (HPE) was added and centrifuged at 12,000 rpm for 1 minute. The flow-through was discarded and the spin column was given a dry spin by centrifugation at 12,000 rpm for 1 minute. The collection tube attached to the spin column was replaced with a new one. To the spin column, 50 µl of elution buffer was added and incubated at room temperature for 3-5 minutes. The spin column was centrifuged at 12,000 rpm for 1 min. The eluate containing the plasmid DNA was stored in a capped polypropylene tube at -20 °C until further use.

PCR primer design: For amplification of the RBD region in the plasmid, primers were designed such a way targeting the 5' and 3' ends of the RBD gene sequence mentioned in Figure 2. The primers designed included necessary restriction sites for cloning purposes. The sequence of the RBD gene and the primers are shown in Figure 2. The primers were ordered from IDT Inc. (Coralville, IA. USA) and their respective data sheets disclosing the properties of forward and reverse primers were displayed in Figure 3.

PCR optimization: To identify the suitable annealing temperature for amplifying the RBD sequence, PCR optimization was performed for a range of annealing temperatures from 50 °C to 60 °C. PCR was performed using Emerald Amp GT PCR Master Mix (2X Premix) (Takara #RR310), forward and reverse primers from IDT and RBD plasmid DNA as template DNA. The required components were added to a 0.2 ml PCR tube (Table 1). The PCR tube was placed in a thermal cycler in which the following PCR protocol was programmed and run to amplify the RBD gene. The protocol was mentioned in Table 2.

Agarose gel electrophoresis: To analyze the quality of the isolated plasmid DNA, the sample was run on 1.5% agarose gel (with 8 µl SYBr Safe Gel Staining Solution). The sample was prepared by mixing 10 µl of plasmid DNA with 2 µl of 6X gel loading buffer. Along with the plasmid DNA, a 1kb ladder was loaded in one of the wells for reference. Since the Emerald Amp GT PCR Master Mix (2X Premix) contained a premixed gel loading buffer, the PCR products were directly loaded into the wells along with a 1kb ladder in one of the wells for reference. The samples were run at 75 volts for 45 minutes. The bands were visualized using a UV lamp.

S.no	PCR Stage	Temperature	Time period
1	Initial Denaturation	94°C	5 min
2	Denaturation	94°C	45 sec
3	Annealing	50°C - 60°C (variable)	30 sec
4	Extension	72°C	30 sec
	Cycles = 30 cycles		
5	Final Extension	72°C	10 min
6	Cooling	4°C	forever

Table 2. PCR protocol.

ISSN: 2583- 2557, *Volume 1, Issue 6, pp18-23. 2023.*

TCABSE-J Interdisciplinary Sciences Journal

5′-ATGAGAGTTCAACCAACAGAATCTATTGTTAGATTTCCAAATATCACCAACTTGTGTCCATTTGGTGAAGTTTTTA
ATGCTACTAGATTCGCTTCTGTTTATGCTTGGAATAGAAAAAGAATCTCTAACTGTGTTGCTGATTATTCTGTTTTGTA
TAACTCTGCTTCTTTCTCTACTTTTAAGTGTTATGGTGTTTCTCCAACAAAATTGAATGATTTGTGTTTCACAAACGTC
TATGCTGATTCTTTTGTTATTAGAGGTGACGAAGTTAGACAAATTGCTCCAGGTCAAACAGGTAAAATTGCTGATTATA
ATTACAAGCTGCCAGATGATTTTACAGGTTGTGTTATTGCTTGGAATTCTAATAATCTGGATTCTAAAGTCGGTGGTAA
TTATAATTACTTGTACAGATTGTTCAGGAAGTCTAATTTGAAACCATTTGAAAGAGACATCTCTACTGAAATATATCAA
GCTGGTTCTACTCCATGTAATGGTGTTGAAGGTTTTAATTGTTACTTCCCATTACAATCTTACGGTTTTCAACCAACAA
ATGGTGTTGGTTATCAACCATATAGAGTTGTTGTTTTATCCTTTGAACTG-3′

Figure 2. RBD template sequence with primers highlighted.

Results and Discussion:

Recovery of bacterial cells from the agar stabs: The plasmid containing RBD gene was purchased from Addgene (#169405). The plasmid contains an ampicillin resistance gene which was used as a selective marker for picking the colonies that contain the plasmid. The plasmid was received in bacterial cells as an agar stab. The cells were grown in LB media containing ampicillin. Since DH5α cells are normally not resistant to ampicillin, the formation of colonies on the LB agar plate containing ampicillin confirms the presence of the plasmid in the bacterial cells (Figure 1).

Isolation of RBD sequence containing plasmid: The quality check of the plasmid extracted was performed by running the plasmid DNA isolated on a 1.5% agarose gel and the bands were visualized using a UV lamp. The results showed that a band was observed above the third band of the 1kb DNA ladder which corresponds to 6 kb. The size of the band obtained was at 6.6 kb size, which matches with the size of the RBD plasmid, Addgene#169405 i.e., 6651 bp. The gel picture displaying the 1kb ladder and RBD plasmid DNA is shown in Figure 3. Since the bands were not very bright, the concentration of the plasmid DNA was assumed to be low. But, a crisp faint band at the required size confirmed the successful extraction of the RBD plasmid.

PCR optimization for RBD amplification: PCR was performed with varying annealing temperatures ranging from 50 °C to 60 °C. All the PCR products were run on a 1.5% agarose gel and the bands were visualized using a UV lamp.

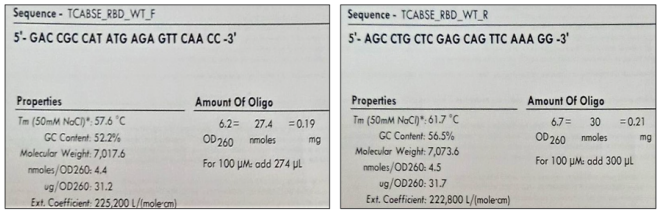

Figure 3. Fact sheets for the primers ordered from IDT Inc.

It was observed that there was successful amplification of the RBD sequence at annealing temperature of 54 °C. The gel picture in Figure 4 shows a very bright crisp band formed above the 500 bp band in the 1 kb ladder. The approximate size of the PCR product was calculated to be 600 bp which matches with the size of the RBD sequence in the plasmid.

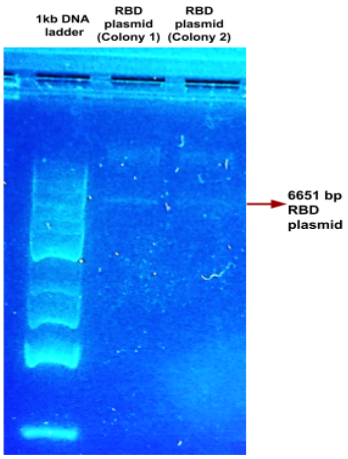

Figure 4. Agarose gel electrophoresis showing the plasmid bands.

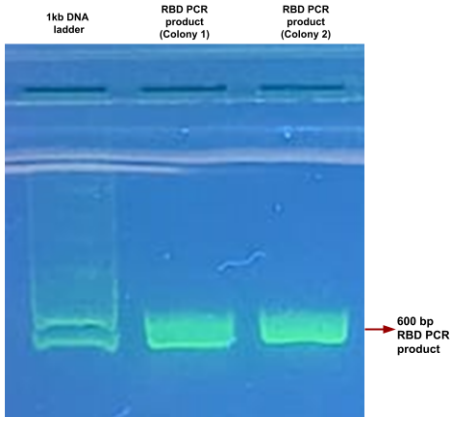

Figure 5. Agarose gel electrophoresis showing the amplified PCR products.

Conclusion and Future directions:

The primers were highly specific resulting in the expected PCR product of correct size. The wild type RBD gene was successfully amplified using PCR as confirmed by the gel electrophoresis. This PCR product can be used for cloning in the future into expression vectors and also as a template for site-directed mutagenesis for protein antigen studies.

Acknowledgements: We thank The Yedidi Institute of Discovery and Education, Toronto for scientific collaborations.

Conflict of interest: The authors declare no conflict of interest in this study. However, this research article is an ongoing project currently at TCABS-E, Visakhapatnam, India.

Acknowledgements: We thank The Yedidi Institute of Discovery and Education, Toronto for scientific collaborations.

Conflict of interest: The authors declare no conflict of interest in this study. However, this research article is an ongoing project currently at TCABS-E, Visakhapatnam, India.

Author contributions: M.V. recovered the bacterial cells from agar stabs, performed PCR optimization, qualitative analysis and wrote the manuscript; S.G. & S.A. performed plasmid isolation, PCR and gel electrophoresis; M.S. assisted M.V. and S.G. in bacterial recovery; M.A. assisted S.G. to repeat PCRs for confirmation; N.M. assisted in gel electrophoresis; B.P. co-supervised S.G.; S.P. co-supervised N.M.; R.S.Y. is the principal investigator, designed the project, trained M.V., S.G., M.S., M.A. and N.M., provided lab space/facilities, edited & finalized manuscript.

References

1. Ravi V, Saxena S, Panda PS. Basic virology of SARS-CoV 2. Indian J Med Microbiol. 2022 Apr-Jun;40(2):182-186. doi: 10.1016/j.ijmmb.2022.02.005. Epub 2022 Mar 14. PMID: 35300895; PMCID: PMC8919811.
2. Tai, W., He, L., Zhang, X. *et al.* Characterization of the receptor-binding domain (RBD) of 2019 novel coronavirus: implication for development of RBD protein as a viral attachment inhibitor and vaccine. *Cell Mol Immunol* 17, 613–620 (2020). https://doi.org/10.1038/s41423-020-0400-4.
3. Lan, J., Ge, J., Yu, J. *et al.* Structure of the SARS-CoV-2 spike receptor-binding domain bound to the ACE2 receptor. *Nature* 581, 215–220 (2020). https://doi.org/10.1038/s41586-020-2180-5
4. Shin HJ, Ku KB, Kim HS, Moon HW, Jeong GU, Hwang I, Yoon GY, Lee S, Lee S, Ahn DG, Kim KD, Kwon YC, Kim BT, Kim SJ, Kim C. Receptor-binding domain of SARS-CoV-2 spike protein efficiently inhibits SARS-CoV-2 infection and attachment to mouse lung. Int J Biol Sci. 2021 Aug 28;17(14):3786-3794. doi: 10.7150/ijbs.61320. PMID: 34671199; PMCID: PMC8495392.
5. Acharya A, Pandey K, Thurman M, Klug E, Trivedi J, Sharma K, Lorson CL, Singh K, Byrareddy SN. Discovery and Evaluation of Entry Inhibitors for SARS-CoV-2 and Its Emerging Variants. J Virol. 2021 Nov 23;95(24):e0143721. doi: 10.1128/JVI.01437-21. Epub 2021 Sep 22. PMID: 34550770; PMCID: PMC8610590.
6. Lim SP. Targeting SARS-CoV-2 and host cell receptor interactions. Antiviral Res. 2023 Feb;210:105514. doi: 10.1016/j.antiviral.2022.105514. Epub 2022 Dec 26. PMID: 36581047; PMCID: PMC9792186.
7. Peng R, Wu LA, Wang Q, Qi J, Gao GF. Cell entry by SARS-CoV-2. Trends Biochem Sci. 2021 Oct;46(10):848-860. doi: 10.1016/j.tibs.2021.06.001. Epub 2021 Jun 7. PMID: 34187722; PMCID: PMC8180548.
8. Muralidar S, Gopal G, Visaga Ambi S. Targeting the viral-entry facilitators of SARS-CoV-2 as a therapeutic strategy in COVID-19. J Med Virol. 2021 Sep; 93(9): 5260-5276. doi: 10.1002/jmv.27019. Epub 2021 May 3. PMID: 33851732; PMCID: PMC8251167.
9. Kang YF, Sun C, Zhuang Z, Yuan RY, Zheng Q, Li JP, Zhou PP, Chen XC, Liu Z, Zhang X, Yu XH, Kong XW, Zhu QY, Zhong Q, Xu M, Zhong NS, Zeng YX, Feng GK, Ke C, Zhao JC, Zeng MS. Rapid Development of SARS-CoV-2 Spike Protein Receptor-Binding Domain Self-Assembled Nanoparticle Vaccine Candidates. ACS Nano. 2021 Feb 23;15(2):2738-2752. doi: 10.1021/acsnano.0c08379. Epub 2021 Jan 19. PMID: 33464829; PMCID: PMC7839421.
10. https://www.addgene.org/169405/

Full figure legends:

Figure 1. LBagar plate showing cell recovery from agar stab. The bacterial cells were successfully recovered from the agar stab by plating on LB agar containing ampicillin as a selection marker. Bacterial lawn indicates the growth of cells containing the desired plasmid that has ampicillin-resistance.

Figure 2. RBD template sequence with primers highlighted. The template DNA that shows the RBD sequence is shown here. The forward primer was designed by taking the bases that are highlighted in yellow color and the reverse primer was designed by considering the sequence that is highlighted in cyan color. The total sequence length for RBD is 600 bp.

Figure 3. Fact sheets for the primers ordered from IDT Inc. The fact sheets for the forward and reverse primers are displayed in the left and right panels, respectively. In addition to the primer sequences, their GC content, melting temperatures, etc. are also given in these sheets.

Figure 4. Agarose gel electrophoresis showing the plasmid bands. Plasmids were isolated from two random colonies and were qualitatively checked on agarose gel. Left most lane

contains the 1kb ladder while the center and right lanes show plasmids of the expected size as indicated in the figure with an arrow.

Figure 5. Agarose gel electrophoresis showing the amplified PCR products. PCR products obtained from the two plasmids were qualitatively checked on agarose gel. The left lane shows 1kb ladder while the center and right lanes show PCR products. Both PCR products were of the same size as pointed by the arrow in the figure.

The Center for Advanced-Applied Biological Sciences & Entrepreneurship (TCABS-E)

Danavaipeta, Rajahmundry; Tel./WhatsApp: 8660301662; Email: tcabse.india@gmail.com

Published by TCABS-E Press on behalf of TCABS-E, Rajamahendravaram. India.